LI
LABORATORY INVESTIGATION
THE BASIC AND TRANSLATIONAL PATHOLOGY RESEARCH JOURNAL
VOLUME 100 | SUPPLEMENT 1 | MARCH 2020

ABSTRACTS

ENDOCRINE PATHOLOGY
(565-611)

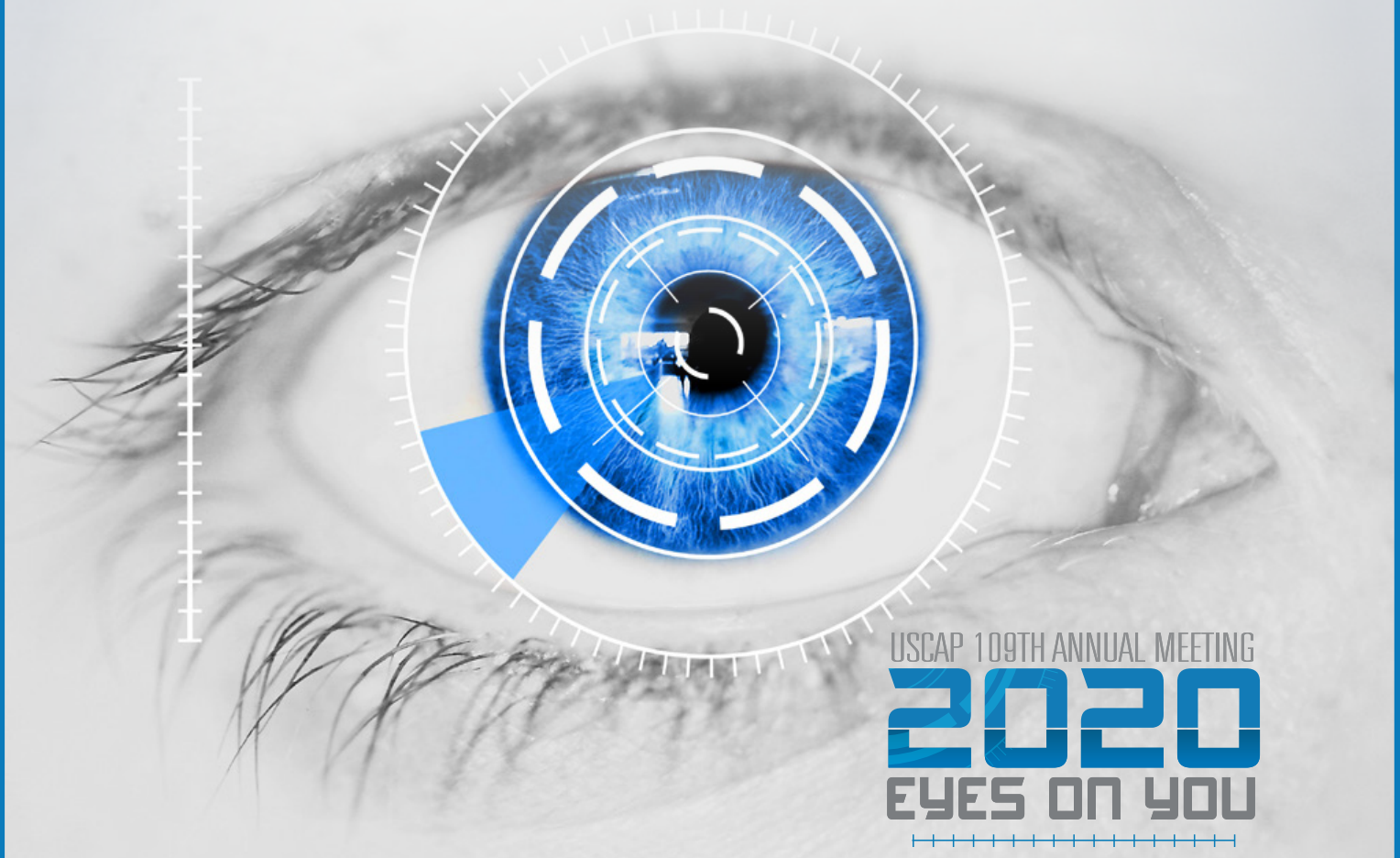

FEBRUARY 29-MARCH 5, 2020

LOS ANGELES CONVENTION CENTER
LOS ANGELES, CALIFORNIA

Published by
SPRINGER NATURE
www.ModernPathology.org

USCAP Creating a Better Pathologist
AN OFFICIAL JOURNAL OF THE UNITED STATES AND CANADIAN ACADEMY OF PATHOLOGY

EDUCATION COMMITTEE

Jason L. Hornick, Chair

Rhonda K. Yantiss, Chair, Abstract Review Board and Assignment Committee

Laura W. Lamps, Chair, CME Subcommittee

Steven D. Billings, Interactive Microscopy Subcommittee

Raja R. Seethala, Short Course Coordinator

Ilan Weinreb, Subcommittee for Unique Live Course Offerings

David B. Kaminsky (Ex-Officio)

Zubair Baloch
Daniel Brat
Ashley M. Cimino-Mathews
James R. Cook
Sarah Dry
William C. Faquin
Yuri Fedoriw
Karen Fritchie
Lakshmi Priya Kunju
Anna Marie Mulligan
Rish K. Pai
David Papke, Pathologist-in-Training
Vinita Parkash
Carlos Parra-Herran
Anil V. Parwani
Rajiv M. Patel
Deepa T. Patil
Lynette M. Sholl
Nicholas A. Zoumberos, Pathologist-in-Training

ABSTRACT REVIEW BOARD

Benjamin Adam
Narasimhan Agaram
Rouba Ali-Fehmi
Ghassan Allo
Isabel Alvarado-Cabrero
Catalina Amador
Roberto Barrios
Rohit Bhargava
Jennifer Boland
Alain Borczuk
Elena Brachtel
Marilyn Bui
Eric Burks
Shelley Caltharp
Barbara Centeno
Joanna Chan
Jennifer Chapman
Hui Chen
Beth Clark
James Conner
Alejandro Contreras
Claudiu Cotta
Jennifer Cotter
Sonika Dahiya
Farbod Darvishian
Jessica Davis
Heather Dawson
Elizabeth Demicco
Katie Dennis
Anand Dighe
Suzanne Dintzis
Michelle Downes
Andrew Evans
Michael Feely
Dennis Firchau
Gregory Fishbein
Andrew Folpe
Larissa Furtado
Billie Fyfe-Kirschner
Giovanna Giannico
Anthony Gill
Paula Ginter
Tamara Giorgadze
Purva Gopal
Anuradha Gopalan
Abha Goyal
Rondell Graham
Alejandro Gru
Nilesh Gupta
Mamta Gupta
Gillian Hale
Suntrea Hammer
Malini Harigopal
Douglas Hartman
John Higgins
Mai Hoang
Mojgan Hosseini
Aaron Huber
Peter Illei
Doina Ivan
Wei Jiang
Vickie Jo
Kirk Jones
Neerja Kambham
Chiah Sui Kao
Dipti Karamchandani
Darcy Kerr
Ashraf Khan
Francesca Khani
Rebecca King
Veronica Klepeis
Gregor Krings
Asangi Kumarapeli
Alvaro Laga
Steven Lagana
Keith Lai
Michael Lee
Cheng-Han Lee
Madelyn Lew
Zaibo Li
Faqian Li
Ying Li
Haiyan Liu
Xiuli Liu
Yen-Chun Liu
Lesley Lomo
Tamara Lotan
Anthony Magliocco
Kruti Maniar
Emily Mason
David McClintock
Bruce McManus
David Meredith
Anne Mills
Neda Moatamed
Sara Monaco
Atis Muehlenbachs
Bita Naini
Dianna Ng
Tony Ng
Michiya Nishino
Scott Owens
Jacqueline Parai
Yan Peng
Manju Prasad
Peter Pytel
Stephen Raab
Joseph Rabban
Stanley Radio
Emad Rakha
Preetha Ramalingam
Priya Rao
Robyn Reed
Michelle Reid
Natasha Rekhtman
Jordan Reynolds
Michael Rivera
Andres Roma
Avi Rosenberg
Esther Rossi
Peter Sadow
Steven Salvatore
Souzan Sanati
Anjali Saqi
Jeanne Shen
Jiaqi Shi
Gabriel Sica
Alexa Siddon
Deepika Sirohi
Kalliopi Siziopikou
Sara Szabo
Julie Teruya-Feldstein
Khin Thway
Rashmi Tondon
Jose Torrealba
Andrew Turk
Evi Vakiani
Christopher VandenBussche
Paul VanderLaan
Olga Weinberg
Sara Wobker
Shaofeng Yan
Anjana Yeldandi
Akihiko Yoshida
Gloria Young
Minghao Zhong
Yaolin Zhou
Hongfa Zhu
Debra Zynger

To cite abstracts in this publication, please use the following format: **Author A, Author B, Author C, et al. Abstract title (abs#). In "File Title."** ***Laboratory Investigation*** **2020; 100 (suppl 1): page#**

565 Topographic Segregation of Genetic Abnormalities during the Neoplastic Progression of Adrenocortical Proliferative Lesions

Fatima Al-Hashimi[1], Salvador Diaz-Cano[2]
[1]Salmaniya Medical Complex, Manama, Bahrain, [2]Queen Elizabeth Hospital Birmingham, Birmingham, United Kingdom

Disclosures: Fatima Al-Hashimi: None; Salvador Diaz-Cano: None

Background: Adrenocortical proliferative lesions reveal kinetic advantages, clonal selection, and vascular angiogenesis during their progression hyperplasia-adenoma-carcinoma. The differential role of genes crucial in the neoplastic progression and their topographic distribution remains both unknown.

Design: We analyzed the adrenal resections performed at a UK tertiary referral center (2009-2014), comprising tumor-like macronodular cortical hyperplasias (TL-ACNH, 8), adenomas (ACA, 8), and carcinomas (ACC, 12). These lesions were evaluated for the primary endocrine syndrome, tumor size, and conventional morphological evaluation including standard Weiss criteria.

Microdissected samples from the peripheral and internal compartments were used for DNA extraction and next-generation sequencing using a 50-gene panel (Qiagen, Hiden, Germany). The mutational burden of each lesion was recorded, and the genetic abnormalities for each locus were categorized by genetic impact according to its severity (low/moderate/high/modifier) and allele frequency. Moderate/high mutated alleles with a frequency higher than 5% were subjected to statistical comparison by non-parametric analysis (Mann-Whitney U-test) and considered significant if $P<0.05$.

Results: TL-ACNH presented with glucocorticoid excess (4) or combined gluco-mineralo-corticoid excess (4), ACA with glucocorticoid excess (6) or mineralocorticoid excess (2), and ACC with plurihormonal excess and mass effect (12). The mutational burden was significantly higher in ACC than the benign counterparts in both compartments: 45 vs. 31.25 and 30.75 for the internal, and 85 vs. 31 and 30 for the peripheral. The internal compartments revealed moderate/high mutations clustered at EGFR, ERBB2, PDGFRA, NRAS, RET, and STK11, NRAS and PDGFRA dominating benign lesion and STK11 predominating in ACC. The peripheral compartments showed differential mutational burden for CTNNB1, PKI3CA, and MET in the ACC only.

Conclusions: Adrenocortical proliferative lesions reveal progressive accumulation of moderate/high mutations during tumor progression and mutational segregation by topographic compartments. Growth factor receptor mutations aggregate in the internal compartment, differentially driven by NRAS and PDGFRA in benign lesions, and additional disruptions at the receptor (PIK3CA and MET) and nuclear (CTNNB1) levels accumulate at the peripheral compartment of ACC.

566 Should Medullary Thyroid Carcinomas Be Graded?

Bayan Alzumaili[1], Bin Xu[2], Philip Spanheimer[3], Nora Katabi[2], Snjezana Dogan[2], Brian Untch[2], Ronald Ghossein[2]
[1]Mt Sinai St Luke's Roosevelt Hospital, New York, NY, [2]Memorial Sloan Kettering Cancer Center, New York, NY, [3]University of North Carolina at Chapel Hill, Chapel Hill, NC

Disclosures: Bayan Alzumaili: None; Bin Xu: None; Philip Spanheimer: None; Nora Katabi: None; Snjezana Dogan: None; Brian Untch: None; Ronald Ghossein: None

Background: Medullary thyroid carcinoma (MTC) is a rare non-follicular cell derived tumors. Despite being morphologically similar to neuroendocrine tumors, no grading system is available. A robust grading system may help better stratify patients at risk for recurrence and death from disease.

Design: One hundred forty-four patients diagnosed as MTC between 1988 and 2018 were subjected to a detailed histopathologic evaluation. Clinical and pathologic data were correlated with disease specific survival (DSS), local recurrence free survival (LRFS), distant metastasis free survival (DMFS) and post-operative serum calcitonin levels.

Results: Median age was 54 years (range: 3-88). Median tumor size was 1.8 cm (range: 0.2-11). Twenty-six (18%) tumors were completely encapsulated. Lymph node metastasis was present in 42 (58%) of cases while distant metastases at presentation were found in 9 (6%) patients. 81% of tumors showed <2 mitosis/10 HPF, 17% 2-9 mitosis /10HPF and 2% showed >=10 mitotic figures/10HPF. Seven (5%) had 5 or more mitosis/10 HPF. Tumor necrosis was present in 30 cases (21%) while vascular invasion occurred in 41 (28%) of tumors. Extra-thyroidal extension was found in 44 (31%) and positive margins were seen in 19 (14%) of specimens. There was a strong correlation between large tumor size and tumor necrosis ($p<0.001$). Median follow up was 39 months. In univariate analysis, larger tumor size, tumor necrosis, high mitotic index (>5/10 HPF), large size of nodal metastasis, high post-operative serum calcitonin predicted DSS, LRFS and DMFS ($p<0.05$). Extra-thyroid extension correlated with DSS and DMFS while positive margins imparted worse DSS ($p<0.05$). The presence of nodal disease was associated with worse LRFS and DMFS ($p<0.05$). In multivariate analysis, tumor necrosis was the only independent prognostic factor associated with local recurrence and death from disease ($p=0.001$). Tumor necrosis and nodal status

were both independent predictor of DMFS (p<0.001 and 0.017 respectively). The 5-year DSS for patients with and without tumor necrosis was 75% and 97% respectively.

Conclusions: Tumor necrosis is the most powerful independent prognostic factor in MTC for DSS and is superior to serum calcitonin and nodal status. This strongly suggest that a grading system based primary on tumor necrosis can be applied to MTC and better stratify patients for additional therapy.

567 Rare Primary Tumors Arising in the Adrenal Gland: A Single Center Review

Francesca Ambrosi[1], Doriana Donatella Di Nanni[2], Maria Giulia Pirini[3], Costantino Ricci[2], Guido Di Dalmazi[2], Vicennati Valentina[2], Donatella Santini[2], Giovanni Tallini[4], Antonio De Leo[2]
[1]S.Orsola-Malpighi Hospital, University of Bologna, Bari, Italy, [2]S.Orsola-Malpighi Hospital, University of Bologna, Bologna, Italy, [3]Department of Pathology, Sant'Orsola-Malpighi Hospital, University of Bologna, Bologna, Italy, [4]University of Bologna School of Medicine, Bologna, Italy

Disclosures: Francesca Ambrosi: None; Doriana Donatella Di Nanni: None; Maria Giulia Pirini: None; Costantino Ricci: None; Guido Di Dalmazi: None; Vicennati Valentina: None; Donatella Santini: None; Antonio De Leo: None

Background: Mostly primary adrenal gland tumors are neoplasms with cortical and medullary origin; however, sarcomas and vascular neoplasms could be anecdotic findings.

Design: We retrospectively reviewed all adrenal specimens submitted to our department of pathology from 2016 to 2019. The aim of the present study is to describe and report histological, immunohistochemical and molecular features of rare primary adrenal gland lesions.

Results: 87 consecutive adrenal gland specimens were analyzed: 44 males and 43 females (median age 57 years, range: 2-85). Primary cortical adrenal lesions were 56/87 (64.4%): 13 (23.2%) hyperplasia, 24 (42.8%) adenoma, 5 (8.9%) carcinoma; 10 (18.9%) pheochromocytoma, 5 (8.9%) myelolipoma and 2 (3.6%) pediatric neuroblastoma. Adrenal metastasis of carcinoma occurred in 19/87 (21.8%) cases.

Thus, 11/87 (12.6%) were rare primary tumors: 2 primary malignant sarcomas (1 Ewing sarcoma and 1 leiomyosarcoma), 1 schwannoma, and 8 benign vascular lesions. (I) The Ewing sarcoma was found in a 25 years old woman, with a previous history of osteosarcoma. Pathological examination revealed a 2.5 cm nodule composed of homogenous, small, round, and blue cells positive for CD99. Molecular analysis was positive for the *EWSR1-FLI1* fusion transcript. (II) The leiomyosarcoma was found in a 59 years old woman with an adrenal mass of 3 cm. The tumor was composed by spindle cells associated with occasional bizarre giant cells, high mitotic index without necrosis. Immunohistochemical staining for muscle markers such as desmin were strongly positive. (III) The adrenal schwannoma was found in a 57 years old woman with a 3 cm adrenal nodule. The tumor showed a microcystic and reticular growth pattern with anastomosing and intersecting strands of spindle cells with eosinophilic cytoplasm distributed around islands of myxoid and hyalinized stroma. The nuclei were round, oval, and tapered and showed inconspicuous nucleoli. Mitotic activity was 3 mitoses/50 high-power fields, pleomorphism and necrosis were absent. (IV) Of 11 vascular lesions, a rare form of sclerosing hemangioma was diagnosed in a 50 years old man, who presented a 2.5 cm nodule of the left adrenal gland and with no previous history of malignancy.

Conclusions: To conclude, pathologists who are familiar with adrenal glands, should take into account soft tissue and vascular neoplasms. These rare findings should be considered in differential diagnosis and could be challenging in distinguishing primary versus metastatic tumors.

568 Epigenomic and Somatic Mutation Profiling of Aggressive Pituitary Neuroendocrine Tumors (PitNETS): Case Series from One Tertiary Referral Center

Sofia Asioli[1], Alberto Righi[2], Doriana Donatella Di Nanni[3], Angelo Corradini[4], Francesca Ambrosi[5], Diego Mazzatenta[6], Matteo Zoli[6], Federica Guaraldi[6], Ricardo Lloyd[7]
[1]University of Bologna, Bologna, Italy, [2]IRCCS Istituto Ortopedico Rizzoli, Bologna, Italy, [3]S.Orsola-Malpighi Hospital, University of Bologna, Bologna, Italy, [4]Pathology Unit, S.Orsola-Malpighi Hospital, University of Bologna, Bologna, Italy, [5]S.Orsola-Malpighi Hospital, University of Bologna, Bari, Italy, [6]IRCCS Istituto delle Scienze Neurologiche di Bologna, Bologna, Italy, [7]University of Wisconsin, Madison, WI

Disclosures: Sofia Asioli: None; Alberto Righi: None; Doriana Donatella Di Nanni: None; Angelo Corradini: None; Francesca Ambrosi: None; Diego Mazzatenta: None; Matteo Zoli: None; Federica Guaraldi: None; Ricardo Lloyd: None

Background: There is little available molecular data about PitNETs with aggressive clinical behavior and more detailed molecular characterization is needed. The aim of the study is to define the molecular typing of aggressive PitNETs and to provide new information to characterize these tumors.

Design: This series was composed of 6 normal pituitary samples, 16 cases of PitNET patients who developed tumor recurrence or disease progression and 12 cases of PitNET patients that remained disease-free after surgical treatment during a minimum of 6 years of follow-up.

Next-generation sequencing for 14 genes known to be involved in PitNETs and DNA methylation analysis evaluated by bisulfite targeted sequencing for *UXT, MAGEA* family, *HDAC6, CDH1, PD-L1, PD-1 (PDCD1), AR, BRCA2, PRC1*were performed in all cases.

Results: Methylation and mutation analyses were feasible in 30 and in 26 cases respectively because of poor DNA quality in some cases. The DNA methylation analysis revealed hypermethylation of UXT in 62%(10/16) PitNETs with recurrence/progression and only 17% (1/7) PitNETs with no recurrence/progression (p=0.04).PitNETs had more consistent epigenetic changes in key genes such as *MAGEA11, TERT,* and *HDAC6* than the non-neoplastic pituitary samples, but there were no statistical differences between patients that developed recurrence/progression and the other patients. From a genetic point of view, the only statistical difference (p=0.047) was observed for*PIK3CA* mutation in 2 cases that developed recurrence/progression and the absence of *PIK3CA* mutation in 5 cases without recurrence/progression. The neoplastic cases showed *NOTCH1* mutation in 69% (9/13), *TP53* mutation in 57% (12/21), *EGFR* mutation in 27% (4/15) cases, but there were no statistical differences between the patients that developed recurrence/progression and the other patient. Six cases of non-neoplastic pituitary tissues did not show methylation in any of the tested genes. In the 12 patients that developed recurrence/progression during follow-up, genetic analyses showed methylation of *UXT* gene and/or mutation of *TP53.*

Conclusions: The detection of this epigenomic and somatic mutation profiling allows for the identification of a subset of more aggressive PitNETs and provides new information that should be useful for prognostic stratification and for planning adjuvant therapy.

569 Immunohistochemistry for the Biotheranostic Markers SSTR2A and CXCR4 in Pheochromocytoma/Paraganglioma

Sarag Boukhar[1], James Howe[1], Thomas O'Dorisio[2], M. Sue O'Dorisio[2], Andrew Bellizzi[1]
[1]University of Iowa Hospitals and Clinics, Iowa City, IA, [2]University of Iowa Hospitals and Clinics

Disclosures: Sarag Boukhar: None; Andrew Bellizzi: None

Background: Our multidisciplinary group has an interest in biotheranostic targets in neuroendocrine neoplasms (NENs). We are opening clinical trials of combined ^{131}I-MIBG and ^{177}Lu-DOTATATE (in advanced midgut neuroendocrine tumors) and ^{177}Lu-Pentixather (in poorly differentiated neuroendocrine carcinomas [NEC] and atypical carcinoid tumors of lung [AC]). We have prospectively performed immunohistochemistry (IHC) for SSTR2A (the target for ^{177}Lu-DOTATATE) on all NENs since 2014 and CXCR4 (the target for ^{177}Lu-Pentixather) on all NECs and ACs since 2017. It was IHC performed on tissue microarrays (TMAs) that validated NECs and identified ACs as target tumor types for our ^{177}Lu-Pentixather trial. Advanced pheochromocytomas/paragangliomas (PHEO/PARA) are often treated with ^{131}I-MIBG. The goal of this study is to define whether these tumors might also benefit from anti-SSTR2A and/or anti-CXCR4 peptide-receptor radionuclide therapy (PRRT).

Design: Immunohistochemistry for SSTR2A (UMB1) and CXCR4 (UMB2) was performed on TMAs of PHEO/PARA (triplicate 1 mm cores). Intensity (0-3+) and extent (0-100%) of staining was evaluated, and an H-score (intensity* extent) was calculated. Results were analyzed relative to age, gender, head and neck (HN) vs thoracoabdominal (TA) location (for PARA), SDHB status (intact/lost), and tyrosine hydroxylase status (positive/negative) using Fisher's exact and Mann Whitney tests ($p<0.05$ considered significant).

Results: SSTR2A was expressed by 85% of 147 PARAs with a mean (median) H-score of 174 (180) and 47% of 131 PHEOs with a mean (median) H-score of 116 (93). Expression was more frequent ($p<0.0001$) and intense ($p=0.0001$) in PARA. Among PARAs, HN tumors (89%) were more frequently positive than TA ones (67%) ($p=0.006$), though with a non-significant difference in H-score. Other than a tendency of SSTR2A-positive PHEOs to occur in older patients (mean/median age 50/50 vs 42/40; $p=0.011$), expression was not related to the other variables analyzed (all p=non-significant). CXCR4 was expressed by 9% of PHEOs and 2% of PARAs ($p=0.008$) with expression weak in both groups (mean/median 23/13 PHEO, 14/13 PARA; $p=0.56$).

Conclusions: PARAs frequently (85%) express SSTR2A, while up to half of PHEOs are positive; expression is typically rather strong. SSTR2A-positive tumors would be attractive candidates for combined ^{131}I-MIBG and ^{177}Lu-DOTATATE PRRT. CXCR4 is infrequently, weakly expressed by these tumors, and patients would not appear to benefit from ^{177}Lu-Pentixather.

570 Global Hypomethylation and Histone Deacetylation in Aggressive Types of Thyroid Carcinoma Detected by Immunohistochemistry and Image Analysis

Andrey Bychkov[1], Thiyaphat Laohawetwanit[2], Sithapong Soontornsit[3], Chaiwat Aphivatanasiri[4], Supinda Koonmee[5], Somboon Keelawat[6]
[1]Kameda Medical Center, Kamogawa, Japan, [2]Thammasat University, Bangsue, Bangkok, Thailand, [3]Institute of Pathology, Thailand, Bangkok, Bangkok, Thailand, [4]Khon Kaen University, Khonkaen, Khonkaen, Thailand, [5]Khon Kaen University, Maung, Khon Kaen, Thailand, [6]Chulalongkorn University, Bangkok, Bangkok, Thailand

Disclosures: Andrey Bychkov: None; Thiyaphat Laohawetwanit: None; Sithapong Soontornsit: None; Chaiwat Aphivatanasiri: None; Supinda Koonmee: None; Somboon Keelawat: None

Background: Epigenetic events are among the major mechanisms involved in neoplastic transformation. These changes include DNA methylation and histone acetylation. Epigenetic drugs demonstrated promising anti-tumor activity in preclinical studies and clinical trials for various malignancies. Single gene and array-wide studies showed that different target genes are involved in epigenetic events in thyroid cancer. However, epigenetic agents are of broad-spectrum and do not target specific genes.

Little is known about patterns of global methylation and histone acetylation in thyroid carcinoma. Our previous studies on differentiated thyroid cancer showed that immunostaining provided more consistent results for evaluating global methylation compared to basic molecular techniques such as LINE-1 and Alu testing. The current study attempts to investigate global methylation and histone acetylation in aggressive types of thyroid cancer, including medullary (MTC), poorly differentiated (PDTC) and anaplastic (ATC) carcinomas employing immunohistochemistry.

Design: We collected 77 cases of aggressive thyroid carcinomas from 2 institutions, including 29 MTCs, 12 PDTCs and, 36 ATCs. Immunostaining with anti-5-methylcytidine, anti-histone 3ac, and anti-histone 4ac antibodies was performed. The intensity and proportion of immunostaining were scored by Aperio ImageScope software (Leica Biosystems, IL). Nuclear scores were evaluated in the neoplastic and non-neoplastic epithelium.

Results: Hypomethylation detected by 5-methylcytidine immunostaining was found in MTC and ATC as compared to their normal counterparts ($p = 0.005$ and 0.01, respectively), whereas PDTC showed no tumor hypomethylation ($p = 0.08$). Deacetylation detected by both histone 3ac and histone 4ac immunostaining was demonstrated in MTC as compared to the normal counterpart ($p = 0.02$ and 0.007, respectively). Similar trend was also found in ATC ($p = 0.002$ and 0.0002 for histones H3 and H4, respectively). In PDTC, deacetylation was found only for histone H3 ($p = 0.04$) but not for histone H4 ($p = 0.14$).

Conclusions: Hypomethylation and deacetylation are found in MTC and ATC compared to the normal follicular epithelium. These finding may implicate further use of epigenetics modifying chemotherapy, particularly methylating and acetylating agents, in MTC and ATC.

571 Hyalinizing Trabecular Tumor of the Thyroid and its Unusual Mimics with Invasive Morphology – An Institutional Series

Andrey Bychkov[1], Ryohei Katoh[2], Takashi Amano[3], Junya Fukuoka[4], Wataru Kitagawa[3], Kiminori Sugino[3], Koichi Ito[5]
[1]Kameda Medical Center, Kamogawa, Japan, [2]Ito Hospital, Shibuya-ku, Japan, [3]Ito Hospital, Tokyo, Japan, [4]Nagasaki University, Nagasaki, Japan, [5]Ito Hospital, Shinagawa-ku, Tokyo, Japan

Disclosures: Andrey Bychkov: None; Ryohei Katoh: None; Takashi Amano: None; Junya Fukuoka: None; Wataru Kitagawa: None; Kiminori Sugino: None; Koichi Ito: None

Background: Hyalinizing trabecular tumor (HTT) of the thyroid got increasing attention due to recent discovery of its genetic signature.

Design: All cases with a diagnosis of HTT, suspicious for HTT, or other thyroid tumors with prominent hyaline change were queried in the pathology database over 2000-2019. Clinical records and follow-up data were analyzed.

Results: We collected 50 cases as per enrollment criteria out of approximately 31.000 thyroid surgicals. After review by 2 thyroid pathologists, 38 cases were diagnosed as HTT (0.12% of all thyroid specimens), 9 cases were non-HTT with typical morphology of follicular adenoma (5), adenomatous nodule (2), or follicular variant PTC (2), and 3 cases were invasive tumors with incomplete HTT phenotype. In 38 HTT cases, the F:M ratio was 18:1, mean age – 53 years, mean size – 22 mm (2–64 mm, with 13/38 sub-cm tumors). Out of 30 nodules sampled preoperatively, only 12 (40%) were cytologically diagnosed or suspected as HTT. Other aspirates were signed out as malignant and suspicious for malignancy (40%), benign (10%), and indeterminate (10%). Histological diagnosis was straightforward in most of the HTT cases, which appeared as trabecular-patterned tumors with thin capsule and frequent pseudonuclear inclusions (Fig. 1a). Chronic lymphocytic thyroiditis was a common background (63%). One case of otherwise typical HTT showed a minute fragment of parenchyma dislocated beyond tumor capsule (Fig. 1b). MIB-1 immunostaining performed in minority of cases (29%) revealed a typical membranous pattern. None of the cases showed adverse outcome on a mean follow-up of 66 months. There were 3 cases initially signed out as invasive HTT, which had a morphology just partially matched with HTT, i.e. trabecular pattern and hyaline deposition but no encapsulation and pseudoinclusions (Fig. 1c-d). These tumors were reminiscent of chromophobe renal cell carcinoma-like thyroid carcinoma, a recently described BRAF-/RAS- entity. Immunostaining revealed TTF1/PAX8+, Tg-, CD117-, weak colloidal iron staining, and low Ki67 index (1–5%). One patient developed several locoregional recurrences.

Figure 1 - 571

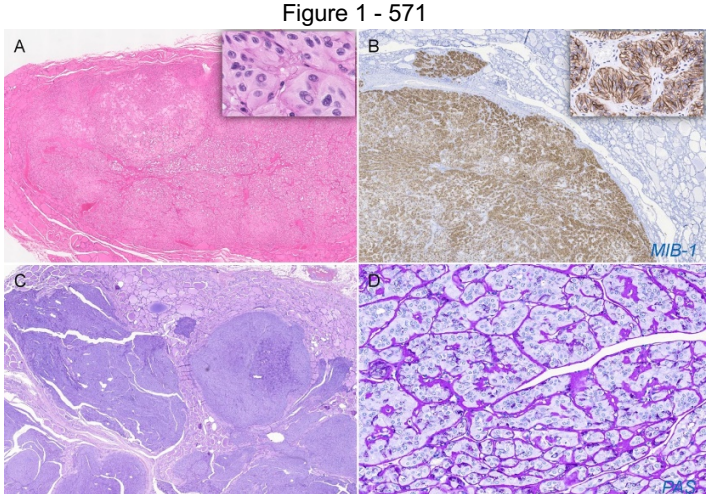

Conclusions: In this largest institutional series to date, we found that HTT is an exceedingly rare tumor with a striking female predilection. Cytological diagnosis is challenging and often confused with PTC, while histology of HTT is usually recognized without difficulties. Typical HTT behaves in benign fashion. We also described a previously underrecognized mimic of HTT with invasive phenotype.

572 Immunophenotypic and Molecular Characterization of Two Cases of Adamantinoma-Like Ewing's Sarcoma of the Thyroid Gland

Kyriakos Chatzopoulos[1], Michael Rivera[1], Rory Jackson[2], Kay Minn[1], Andre Oliveira[1], Kevin Halling[1], Kandelaria Rumilla[1]
[1]*Mayo Clinic, Rochester, MN*

Disclosures: Kyriakos Chatzopoulos: None; Michael Rivera: None; Rory Jackson: None; Kay Minn: None; Andre Oliveira: None; Kevin Halling: None; Kandelaria Rumilla: None

Background: Adamantinoma-like Ewing's sarcoma is a rare malignancy of unclear histogenesis, very rarely reported in the thyroid gland. Differential diagnosis can be challenging due to its rarity and poorly differentiated morphology. We evaluated the phenotype and molecular findings of two cases diagnosed in our institution.

Design: Surgical pathology material from two patients diagnosed with adamantinoma-like Ewing's sarcoma of the thyroid gland was retrieved from consultation files and reviewed by two expert endocrine pathologists. Immunohistochemistry (IHC) was performed for: CK7, CK20, CK5/6, keratins AE1/AE3, CAM5.2, CD45, CD20, CD5, CD99, chromogranin, synaptophysin, calcitonin, thyroglobulin, PAX8, TTF1, S100, p40, p63, p16, NUT, desmin, ER, FLI1, INI1, desmin and myogenin. HPV DNA in situ hybridization (ISH) was performed for family 16 viruses including types 16, 18, 31, 33 and 51. *EWSR1* rearrangement status was evaluated by FISH, RT-PCR and RNA sequencing.

Results: The patients were a 49 year-old-man and a 30 year-old woman. Morphologically both were high grade malignancies with trabecular and nested architecture, abundant necrosis and brisk mitotic activity. Except for a few areas containing entrapped thyroid follicles, the tumors were morphologically homogeneous without areas suggestive of a low grade component. IHC showed consistent expression of keratins (AE1/AE3 and CAM5.2), particularly of high molecular weight (CK5/6), as well as diffuse reactivity for p40, p63 and p16. CD99 was strongly expressed only in the tumor of the 49-year-old man and was weak and focal in the tumor of the 30 year-old woman. INI1 was retained in both lesions. All other stains, as well as high risk HPV DNA ISH, were negative. Break apart FISH was indicative of *EWSR1* (22q12) rearrangement. We identified the *EWSR1-FL1* fusion transcript by RT-PCR and RNA sequencing.

Conclusions: Adamantinoma-like Ewing's of the thyroid gland is a rare malignancy which can morphologically resemble, among others, poorly differentiated squamous cell carcinoma, and undifferentiated carcinoma. Detection of *EWSR1* rearrangement should be considered if morphology and the initial rounds of immunohistochemistry raise suspicion for the diagnosis.

573 Can a Histologic Pattern Predict ACTH Production in Pheochromocytoma?

Zachary Chelsky[1], Maria Tretiakova[1]
[1]*University of Washington, Seattle, WA*

Disclosures: Zachary Chelsky: None; Maria Tretiakova: None

Background: ACTH production by pheochromocytomas is a rare finding that is not always clinically apparent. In ACTH-producing pheochromocytomas, most ACTH immunostaining is focal, thus suggesting that a unique population of tumor cells is responsible for production of the hormone. To date, no studies have attempted to correlate ACTH production with histology in pheochromocytomas. We aimed to identify morphologic patterns that could correlate with ACTH production.

Design: Two recent cases of ACTH-producing pheochromocytomas were identified and ACTH immunostaining was performed. ACTH positive areas were compared with each other and to ACTH negative areas to identify a common histologic pattern. A tissue microarray of 21 cases of pheochromocytomas and paragangliomas was then ACTH stained to further correlate the histologic patterns

Results: Two cases with clinically suspected ACTH-producing pheochromocytomas included case 1 with 60% ACTH immunoreactivity (Figures 1A and 1D) and case 2 with 25-30% ACTH immunoreactivity of the tumor (Figures 1B ad 1E). Regions of tumor positive for ACTH demonstrated a diffuse growth pattern, increased cellularity, cytoplasmic clearing with foamy or vacuolated cytoplasm (reminiscent of adrenocortical cells rather than medullary cells), as well as areas with fibrosis, hemorrhage and abundant hyaline globules. Nine out of 21 cases included in the tissue microarray expressed ACTH (range 1-60% positive cells), and ACTH was present in areas with the histologic patterns described above. ACTH negative regions of these tumors and of ACTH negative pheochromocytomas had classic zellballen architecture (Figures 1C and 1F). Six cases in the microarray involved metastatic or recurrent disease. ACTH was expressed in 3 of these cases with a combination of ACTH positive and negative primary and metastatic tumors.

Figure 1 - 573

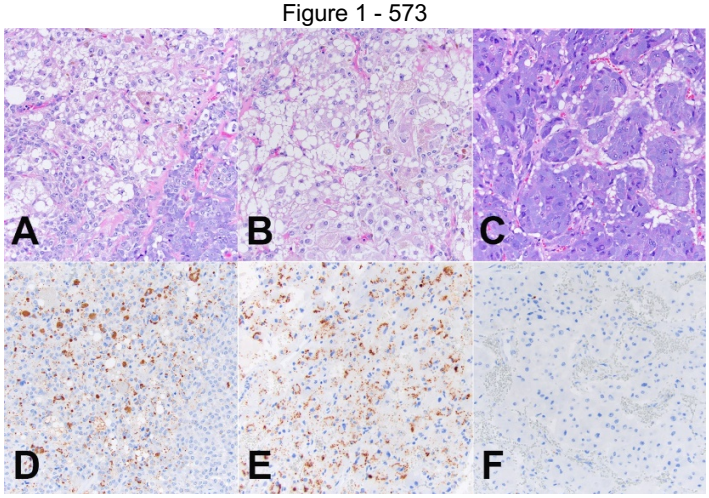

Conclusions: We propose that a unique histologic pattern exists that correlates with ACTH production. Our results suggest that staining for ACTH should be performed in regions of tumor containing certain histologic features in order to avoid missing ACTH immunoreactivity. In addition, our study suggests that ACTH expression in pheochromocytoma shows significant intratumor and intrapatient variation.

574 Clinicopathologic Features of BRAF V600E-Mutant Anaplastic Thyroid Carcinoma

Tiffany Chen[1], Kristine Wong[2], Justine Barletta[3]
[1]Brookline, MA, [2]Brigham and Women's Hospital, Boston, MA, [3]Brigham and Women's Hospital, Harvard Medical School, Boston, MA

Disclosures: Tiffany Chen: None; Kristine Wong: None; Justine Barletta: None

Background: Anaplastic thyroid carcinoma (ATC) is both morphologically and molecularly heterogeneous. Treatment with a BRAF inhibitor alone or in combination with a MEK inhibitor may be considered for *BRAF*-mutant ATC. We evaluated a cohort of ATC to evaluate the rate of *BRAF* V600E mutation and the clinicopathologic features of *BRAF* V600E-mutant ATC.

Design: We identified all consecutively resected ATC from 2003 to 2019. All tumor slides were evaluated for the presence of a precursor lesion, percentage of the anaplastic component, and morphology of the anaplastic component (sarcomatoid, pleomorphic giant cell, epithelioid, squamous). A p63 immunohistochemical stain was performed on all cases to evaluate for squamous differentiation. For cases with a mixed morphology, the predominant morphology was recorded. *BRAF* V600E mutation status was determined by either *BRAF* V600E mutation-specific immunohistochemistry or targeted next-generation sequencing.

Results: Our cohort included 36 ATC, including 12 (33%) that arose from papillary thyroid carcinoma (PTC), 7 (19%) from follicular thyroid carcinoma, 2 (6%) from Hurthle cell carcinoma, and 6 (17%) from poorly differentiated thyroid carcinoma. 9 (25%) cases lacked a precursor lesion. The anaplastic component comprised a minor component of the tumor (≤10%) in 8 (22%) cases. The predominant morphology was

sarcomatoid in 13 (36%), pleomorphic giant cell in 3 (8%), epithelioid in 15 (42%), and squamous in 5 (14%) cases. 14 (39%) tumors harbored a *BRAF* V600E mutation. *BRAF* V600E-mutant tumors were more frequently associated with PTC (79% versus 5%, $p<0.0001$) and more frequently showed either overt squamous differentiation histologically or p63 positivity (43% versus 9%, $p=0.036$).

Conclusions: Our findings suggest that morphological features, such as squamous differentiation and the presence of a PTC precursor lesion, may be predictors of *BRAF* V600E mutation status in ATC.

575 Intracapsular (Eggshell) Calcification as a Harbinger of Malignancy in Follicular-Derived Thyroid Tumors

Ying-Hsia Chu[1], Vania Nose'[2], Peter Sadow[2], Yanping Wang[3], Qiqi Yu[4], Rong Hu[5], Ricardo Lloyd[6]
[1]Massachusetts General Hospital, Harvard Medical School, Cambridge, MA, [2]Massachusetts General Hospital, Harvard Medical School, Boston, MA, [3]UW Hospital and Clinics, Madison, WI, [4]University of Wisconsin, Madison Hospital and Clinics, Madison, WI, [5]Madison, WI, [6]University of Wisconsin, Madison, WI

Disclosures: Ying-Hsia Chu: None; Vania Nose': None; Peter Sadow: None; Yanping Wang: None; Qiqi Yu: None; Rong Hu: None; Ricardo Lloyd: None

Background: Calcification is common within the thyroid gland and occurs in a number of non-neoplastic and neoplastic settings. Although it has been suggested that the incidence of malignancy in thyroid nodules containing calcifications is higher than in the average thyroid nodule, the histopathologic patterns and localization of calcification has usually not been associated with specific subtypes of thyroid malignancies except for psammomatous calcifications in papillary thyroid carcinomas (PTC). Despite the recognition and identification of psammoma bodies in PTC, the incidence and association of other calcification types is unclear, as reporting about calcifications is not a standard component of pathology reports.

Design: We analyzed hematoxylin and eosin stained sections of 464 cases of follicular-derived thyroid tumors including follicular adenomas (FA) (N=204), follicular carcinomas (FC) (N=113), Hurthle cell carcinomas (HC) (N=32), and encapsulated follicular variant of papillary thyroid carcinomas (EFVPTC) (N=115) for the presence of intracapsular (eggshell) calcifications (Figures 1 and 2) from two institutions. The presence of psammomatous calcifications in classical PTC and dystrophic calcifications present in non-capsular regions of tumors were not included in the study. Cases from each institution were reviewed by two observers and disagreements were reviewed with a multi-headed microscope.

Results: Intracapsular calcification was present in 5.4% of FA, 25.7% of FC, 28.1% of HC and 8.7% of FVPTCs ($P<0.05$ for FC vs. FA and HC vs. FA). The extent of vascular invasion was not related to the degree of capsular calcification.

Figure 1 - 575

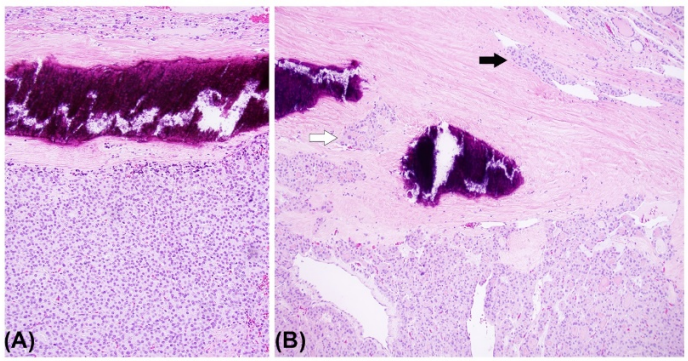

Figure 1: (A) Follicular carcinoma with capsular calcification (B) Capsular (white arrow) and vascular (black arrow) invasion can be seen percolating through the calcified capsule.

Figure 2 - 575

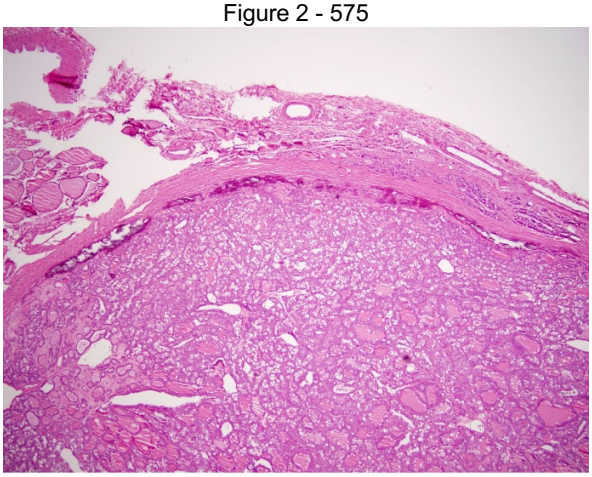

Figure 2: Papillary thyroid carcinoma, follicular variant, with capsular calcification

Conclusions: Follicular-derived thyroid tumors with intracapsular (eggshell) calcifications are more likely to represent malignant neoplasms in follicular and Hurthle cell thyroid neoplasms. Some cases of encapsulated FVPTC may also contain intracapsular (eggshell) calcifications. These findings should encourage pathologists to perform further examination of thyroid neoplasms in which intracapsular calcification is present but no overt vascular or capsular invasion is noted.

576 Patient and Clinician-Driven Requests for Thyroid Nodule Reappraisal in the NIFTP Era: A Prospective Experience of Retrospective Review

Vincent Cracolici[1], Linwah Yip[1], Esra Karslioglu-French[1], Yuri Nikiforov[1], Raja Seethala[2]
[1]*University of Pittsburgh Medical Center, Pittsburgh, PA,* [2]*University of Pittsburgh School of Medicine, Pittsburgh, PA*

Disclosures: Vincent Cracolici: None; Linwah Yip: None; Esra Karslioglu-French: None; Yuri Nikiforov: None; Raja Seethala: None

Background: With the introduction of non-invasive follicular thyroid neoplasm with papillary-like nuclear features (NIFTP) as a diagnostic category, patients and clinicians alike have requested reassessment when tumors were previously designated as follicular variant of papillary thyroid carcinoma (FVPTC). Reclassification may allow for de-escalation of follow-up and testing. We describe our prospective experience with patient and clinician driven re-review of nodules that may potentially be reclassified as NIFTP under current, strict criteria.

Design: Patient and/or clinician driven requests for tumor reassessment were tracked prospectively (2016 – present). Patient demographics and clinical follow-up were obtained. The tumors were re-assessed under strict modifications of original NIFTP criteria (used institutionally since 2016; formalized in 2018 - PMID: 29902314). For the purposes of this study, oncocytic features were considered exclusionary for NIFTP.

Results: Requests were received for 111 patients (131 thyroid nodules). 123 nodules were considered for reclassification given the availability of glass slides and/or pathology reports. 33 (26.8%) nodules were only subject to report review as exclusionary criteria were present in the gross description or diagnosis. No patient has had recurrence, though six (4.8%) have stable neck nodules.

27 (22%) cases were reclassified as NIFTP. All cases reclassified as NIFTP were originally diagnosed as FVPTC or EFVPTC. Original diagnoses for cases not reclassified as NIFTP included 84 EFVPTC (including 9 oncocytic cases and 3 cases with capsular invasion), 11 cases of conventional PTC, and 1 oncocytic follicular adenoma. See Table 1 for comprehensive assessment.

Incomplete capsule submission excluded 25 (26%) cases from reclassification. 32 (33.3%) cases harbored papillae/conventional foci. 17 (17.7%) cases had capsular thyroid parenchymal invasion and 17 (17.7%) cases were oncocytic. 8 (8.4%) cases had solid growth and 4 (4.4%) had increased mitoses (>3/10 hpf). 1 case had a tall cell component, and 1 case had a positive surgical margin. 1 case had inadequate nuclear features for NIFTP. 8 (8.4%) cases had multiple exclusionary features.

Table 1: Clinicopathologic Features of Reassessed Thyroid Nodules

	Reclassified as NIFTP *27 nodules from 27 patients*	Not Reclassified as NIFTP *96 nodules from 82 patients*
Patient Age (years), p=0.5 *Mean* *Median* *Range*	48.7 49 32-74	47.1 47 18-77
Sex (n), p=0.18	4 male, 23 female	20 male, 64 female
Radioactive Iodine Therapy (n)	3 (11.5%)	40 (48%)
Surgery (n) *Total Thyroidectomy* *Hemithyroidectomy* *Lobectomy* *Central Lymph Node Dissection*	13 9 5 1	40 23 19 12
Mean Follow-up Time (months)	67.1	84.5
Tumor Size (cm) p=1.0 *Mean* *Median* *Range*	2.3 2.0 0.4-5.3	2.3 2.0 0.1-6.9

Conclusions: Only 22% of cases re-reviewed by clinician or patient request are actually reclassified as NIFTP when strict criteria are applied. There are no significant clinical, or demographic differences between cases that are reclassified as NIFTP, and those that are not, and neither group showed recurrence.

577 Clinical Significance of TERT Promoter and TP53 Mutations in Thyroid Nodules with Indeterminate Cytology

Dominick Guerrero[1], Pablo Valderrabano[2], Valentina Tarasova[1], Bryan McIver[1], Bruce Wenig[1], Juan Hernandez-Prera[1]
[1]*Moffitt Cancer Center, Tampa, FL,* [2]*Hospital Universitario Ramón y Cajal, Madrid, Spain*

Disclosures: Dominick Guerrero: None; Pablo Valderrabano: None; Valentina Tarasova: None; Bryan McIver: *Speaker*, Sonic Healthcare USA; Bruce Wenig: None; Juan Hernandez-Prera: None

Background: TERT and TP53 mutations are reported in aggressive thyroid cancers such as poorly differentiated (PDTC) and anaplastic thyroid carcinomas (ATC), and they confer an increased risk of tumor recurrence and tumor-related mortality to well-differentiated cancers (WDTC). With the increased use of oncogene panel testing in thyroid cytology, these alterations are also encountered in the presurgical evaluation of cytologically indeterminate thyroid nodules and their clinical significance in this context is unknown. We explored the clinicopathologic features of indeterminate thyroid nodules with these mutations.

Design: Our database of thyroid nodules subjected to Thyroseq was interrogated to identify nodules with TERT and/or TP53 mutations. Thyroid cancers with the these mutations found by FoundationOne were retrieved for comparison.

Results: 11 out of 431 nodules tested by Thyroseq showed TERT (6) and TP53 (5) mutations. Cytological diagnoses were 4 Bethesda III, 6 Bethesda IV, 1 Bethesda VI. 8 cases had total thyroidectomy. Among resected TERT mutant nodules (n=4): 1 with BRAFV600E mutation was a metastatic melanoma; 1 with RAS mutation was as follicular adenoma (FA); 2 nodules with EIF1AX/RAS mutations were widely invasive follicular carcinoma (FC). The FCs were large tumors (6.2 and 4.6 cm), 1 had bulky nodes and 1 had distant metastasis at postoperative evaluation. Among resected TP53 mutant nodules (n=4), 1 with RAS mutation was a FA; the remaining 3 cases with isolated TP53 mutations were 2 oncocytic FAs and 1 adenomatoid nodule. 2 patients with isolated TERT mutations and 1 patient with TP53 and RAS mutations are under active surveillance due to comorbidities and are stable on follow-up.18 out of 32 cases analyzed by FoundationOne, had TERT and/or TP53 mutations. All cases were aggressive cancers (10 ATC, 2 PDTC and 6 WDTC with distant metastasis) with multiple mutations and 7 patients died of the disease.

Conclusions: TERT and TP53 mutations are rare events in cytologically indeterminate thyroid nodules and often associated with indolent behavior unless multiple concomitant mutations are identified. In contrast, TERT and TP53 mutations are highly prevalent in clinically aggressive tumors. The role of TERT and TP53 mutations as a predictor of unfavorable outcomes in thyroid cancer depends on which population is interrogated and should be carefully extrapolated to thyroid nodules with indeterminate cytology.

578 Molecular Determinants of Thyroid Nodules with Indeterminate Cytology and RAS Mutations

Juan Hernandez-Prera[1], Pablo Valderrabano[2], Jordan Creed[1], Janis de la Iglesia[1], Robbert Slebos[1], Barbara Centeno[1], Bruce Wenig[1], Travis Gerke[1], Christine Chung[1]
[1]Moffitt Cancer Center, Tampa, FL, [2]Hospital Universitario Ramón y Cajal, Madrid, Spain

Disclosures: Juan Hernandez-Prera: None; Pablo Valderrabano: None; Jordan Creed: None; Janis de la Iglesia: None; Robbert Slebos: None; Barbara Centeno: None; Bruce Wenig: None; Travis Gerke: None; Christine Chung: None

Background: *RAS* gene family mutations are the most prevalent in thyroid nodules with indeterminate cytology and are present in a wide spectrum of histological diagnoses ranging from adenomatoid nodules to aggressive and metastatic thyroid cancers. We evaluated differentially expressed genes and signaling pathways across the histological/clinical spectrum of *RAS*-mutant nodules to determine key molecular determinants associated with a high risk of malignancy.

Design: Sixty-one thyroid nodules with *RAS* mutations were identified. Based on the histological diagnosis and biological behavior, the nodules were grouped into five categories indicating their degree of malignancy: non-neoplastic appearance, benign neoplasm, indeterminate malignant potential, low-risk cancer, or high-risk cancer. Gene expression profiles of these nodules were determined using NanoString PanCancer Pathways and IO360 panels, and Angiopoietin-2 level was determined by immunohistochemical staining.

Results: Unsupervised cluster analysis exhibited a relatively homogeneous expression pattern with no discrete groups. The analysis of genes that were differentially expressed in the 5 categories as supervising parameters unearthed a significant correlation between the degree of malignancy and genes involved in cell cycle and apoptosis (*BAX, CCNE2, CDKN2A, CDKN2B, CHEK1, E2F1, GSK3B, NFKB1*, and *PRKAR2A*), *PI3K* pathway (*CCNE2, CSF3, GSKB3, NFKB1, PPP2R2C*, and *SGK2*), and angiogenesis (*ANGPT2* and *DLL4*). The expression of Angiopoietin-2 by immunohistochemistry also showed the same trend of increasing expression from non-neoplastic appearance to high-risk cancer (p-value <0.001).

Conclusions: The gene expression analysis of *RAS*-mutant thyroid nodules suggests increasing upregulation of key oncogenic pathways depending on their degree of malignancy and supports the concept of a stepwise progression that starts in early thyroid lesions that morphologically have a non-neoplastic appearance such as adenomatoid nodules. The ANGPT2 expression as a diagnostic biomarker warrants further evaluation.

579 Phenotypic, Proliferative, and Genomic Diversities in Pituitary Carcinomas: A Proposal for "Pituitary neuroendocrine neoplasms (PitNENs) with malignant potential"

Chie Inomoto[1], Robert Osamura[2], Kenichi Oyama[3], Shigeyuki Tahara[4], Akira Matsuno[5], Akira Teramoto[4]
[1]Isehara, Japan, [2]Nippon Koukan Hospital, Kawasaki, Japan, [3]Teikyo University School of Medicine, Itabashi, Japan, [4]Nippon Medical School, Tokyo, Japan, [5]Teikyo University School of Medicine, Tokyo, Japan

Disclosures: Chie Inomoto: None; Robert Osamura: None; Kenichi Oyama: None; Shigeyuki Tahara: None; Akira Matsuno: None; Akira Teramoto: None

Background: The pituitary carcinoma is rare and is strictly defined as a tumor of adenohypophyseal cells that metastasizes craniospinally or is associated with systemic metastases (WHO 2017). Recently, pituitary adenomas and carcinomas are regarded as neuroendocrine neoplasms (NENs) by their common expression of the Insulinoma-associated protein1(INSM1) (USCAP 2019). Our study is aimed at to elucidate how the classification and grading system of NEN in the pancreas and digestive system(WHO 2017,2019) can be applied to those in the pituitary glands, particularly pituitary carcinomas.

Design: Total seven cases of pituitary carcinomas were studied for the morphological, hormonal, phenotypic, proliferative and genomic characteristics by Immunohistochemically. Immunohistochemical staining was done for pituitary hormones and subunits, Ki-67 indices(%), p53 indices(%), Rb1(+ or -), ATRX/DAXX(+ or -). Two cases revealed metastases in the liver (Case 2, 3). The other cases showed intracranial metastases or meningo-spinal spread.

Results: Morphologically, the tumor cells were diverse showing Crooke change, marked pleomorphism, small poorly differentiated or vacuolated cytoplasm. Immunohistochemically, ACTH was positive in three cases (Cases 2,3,5), one with Crooke change (Case 2), and the other with marked pleomorphism (Case 3). PRL was positive in two cases (Case 4, 6). The remaining cases (Case 1, 7) were negative for pituitary hormones or subunits. Ki-67 index higher than 20%(NET G3 or NEC) were 4 cases, Ki-67 index 2-20%(NET G2) were three cases. p53 was strongly positive (more than 50% of the tumor cells), Case 3 and Case 5(metastatic site), both were positive for ACTH. But Rb1 and ATRX/ADXX were retained. Remaining cases showed p53 less than 3% and weak. One case (Case 1) showed high (74.6%) Ki-67 index with poorly differentiated pattern, but negative p53 and positive Rb, ATRX/DAXX.

Conclusions: These data suggest that malignant transformation is diverse and can occur with p53 mutation in ACTH producing PitNENs, or without p53 mutation in the other PitNENs. Crooke cell, pleomorphic, large cell types of ACTH-producing PitNENs may suggest malignant potential. Small tumor cell in PitNENs sometimes produce PRL and those with higher Ki-67 indices(74.6%,27.8%,40.2%) should be also potential for malignant behavior. These various PitNENs should be categorized under the terminology "PitNENs with malignant potential". Classification and grading system(WHO 2017,2019) NET, NEC may not be equally applicable to PitNENs.

580 RAS Mutations Detected in Fine Needle Aspiration Biopsy of Thyroid Nodules Strongly Correlate with Benign Histologic Diagnoses

Daniel Johnson[1], Tatjana Antic[2], Ward Reeves[2], Sara Jackson[3], Christina Narick[3], David Sarne[2], Peter Angelos[2], Sydney Finkelstein[3], Nicole Cipriani[2]
[1]Northwestern University Feinberg School of Medicine, Chicago, IL, [2]The University of Chicago, Chicago, IL, [3]Interpace Diagnostics, Pittsburgh, PA

Disclosures: Daniel Johnson: None; Tatjana Antic: None; Ward Reeves: None; Sara Jackson: *Employee*, Interpace Diagnostics; Christina Narick: *Employee*, Interpace Diagnostics; David Sarne: None; Peter Angelos: None; Sydney Finkelstein: *Employee*, Interpace Diagnostics; Nicole Cipriani: None

Background: Molecular testing on fine needle aspiration (FNA) of thyroid nodules has become a standard component of preoperative evaluation. A majority of thyroid tumors can be divided genetically into BRAF-V600E-like (papillary carcinoma) and RAS-like (follicular neoplasms including follicular adenoma, follicular carcinoma, and NIFTP). NRAS, HRAS, and KRAS mutations occur in both benign and malignant follicular neoplasms as well as in nodules that appear morphologically hyperplastic. We examined FNA molecular results from a commercial combined miRNA profiling and DNA next generation sequencing test in the context of surgical outcomes.

Design: All cytologically indeterminate thyroid FNA specimens (atypia of undetermined significance (AUS), follicular lesion of undetermined significance (FLUS), suspicious for follicular neoplasm (SFN)) sent from our tertiary academic institution for routine clinical molecular testing to Interpace (Parsippany, NJ) from 2016 to 2019 were identified. Molecular results, clinical, and surgical pathology follow-up was recorded.

Results: Of 75 identified cases (10 AUS, 54 FLUS, 11 SFN), 24 (32%) were resected (Table 1). 50 (67%) were classified as molecular benign; all 9 that underwent resection (8 FLUS, 1 SFN) were benign. 25 (33%) were classified as non-benign; 19 had RAS mutation (3 AUS, 13 FLUS, 3 SFN); of these, all 11 that underwent resection were benign, 8 which also had positive miRNA profiling. The remaining 4 cases that underwent surgical resection were 2 PTC (1 AUS with positive miRNA only, 1 SFN with BRAF V600E and TERT promoter mutations), 1 FTC (SFN with GNAS and PTEN mutations and negative miRNA, metastatic to the sinus), and 1 MTC (SFN with molecular

favoring MTC). Of the 51 (68%) patients that did not undergo resection, no clinical evidence of disease progression or metastasis was seen in any patient classified as benign or with RAS mutation.

Category	n	Interpace Benign	Benign Resected	Interpace non-Benign	non-Benign Resected
III (FLUS microfollicular architecture)	54	41 (76%)	8 -> 8 Benign	13 (24%) 6 RAS, miR- 7 RAS, miR+	5 ->1 Benign ->4 Benign
III (AUS nuclear atypia)	10	6 (60%)	None	4 (40%) 1 RAS, miR- 2 RAS, miR+ 1 miR+	4 ->1 Benign ->2 Benign ->1 PTC
IV (SFN)	11	3 (27%)	1 -> 1 Benign	8 (72%) 2 RAS, miR+ 1 RAS, miR- 1 miR+ 1 Favor MTC 1 BRAF VE + TERT 1 GNAS, PTEN, miR- 1 TERT, miR-	6 ->2 Benign ->1 Benign -> Not Resected ->1 MTC ->1 PTC ->1 FTC met to bone -> Not Resected

Conclusions: Performance of molecular testing on FNA decreased the rate of surgical intervention in indeterminate nodules by 68 percentage points. Rates of benign molecular results were high (67% overall; 76% of FLUS) and lowest for SFN (27%). Isolated RAS mutation (regardless of positive or negative miRNA) was highly likely to be benign upon surgical resection. The risk of malignancy anticipated by Interpace for RAS-mutated nodules ranged from 25-85%. Actual rates of malignancy may be lower, and close observational management could be considered in these patients.

581 Molecular Correlates of Clinical Outcomes in Differentiated Thyroid Carcinoma Patients with Distant Metastasis

Chan Kwon Jung[1], Seung-Hyun Jung[2], Sora Jeon[3], Young Mun Jeong[4], Yourha Kim[3], Sohee Lee[5], Ja-Seong Bae[5], Yeun-Jun Chung[6]

[1]The Catholic University of Korea, Seoul St. Mary's Hospital, Seoul, Korea, Republic of South Korea, [2]Cancer Evolution Research Center, College of Medicine, The Catholic University of Korea, Seoul, Korea, Republic of South Korea, [3]Cancer Research Institute, College of Medicine, The Catholic University of Korea, Seoul, Korea, Republic of South Korea, [4]Department of Biomedicine & Health Sciences, College of Medicine, The Catholic University of Korea, Seoul, Korea, Republic of South Korea, [5]Department of Surgery, College of Medicine, The Catholic University of Korea, Seoul, Korea, Republic of South Korea, [6]Department of Microbiology, College of Medicine, The Catholic University of Korea, Seoul, Korea, Republic of South Korea

Disclosures: Chan Kwon Jung: None; Yeun-Jun Chung: None

Background: Although most differentiated thyroid cancers (DTC) are indolent, DTCs with distant metastasis show poor prognosis. However, there are no markers for risk of distant metastasis and prognosis. We aimed to develop a genetic classifier for predicting prognosis of DTC patients with distant metastasis.

Design: Targeted deep sequencing of 157 cancer-related genes was performed for 47 DTCs with distant metastasis. Candidate mutations were validated with independent thyroid cancer samples using digital PCR.

Results: Five mutations were detected in over 10% of the metastatic DTCs; *TERT* promoter (55%), *BRAF* (51%), *PLEKHS1* promoter (13%), *NRAS* (11%), and *STK11* (11%). In an independently collected DTCs without metastasis (n=75), no *PLEKHS1* promoter mutation was found, suggesting it might be metastasis-specific. *PLEKHS1* promoter mutations were more common in radioactive iodine (RAI)-refractory cases (P = 0.022). In multivariate analysis, bone metastasis (adjusted OR [aOR] 14.68, P = 0.003) and at least one mutation in either *TERT* promoter, *PLEKHS1* promoter or *TP53* (aOR 9.02, P = 0.012) remained significantly associated with RAI-refractoriness. We developed a genetic classifier consisting of *BRAF*, *RAS*, *TERT* promoter, *PLEKHS1* promoter, and *TP53* for categorizing prognosis of DTC with metastasis. In the poor-prognosis group, 67% of the patients were RAI-refractory and death occurred in 23% during the follow-up. In the intermediate-prognosis group, 40% were RAI-refractory, but no death occurred. In the good-prognosis group, all patients were RAI-responsive and no death occurred.

Conclusions: *PLEKHS1* promoter mutation is a novel genetic marker of aggressive DTC. Our genetic classifier can be useful for treatment selection in DTC patients with distant metastasis.

582 NET G3: Clinicopathological and Diagnostic Features in a Consultation Case Series

Atsuko Kasajima[1], Bjorn Konukiewitz[2], Anna Schlitter[3], Wilko Weichert[4], Günter Klöppel[5]
[1]Munich, Bayern, Germany, [2]Munchen, Germany, [3]Munich, Germany, [4]Institute of Pathology, Muenchen, Germany, [5]Technical University Munich, Munich, Bavaria, Germany

Disclosures: Atsuko Kasajima: None

Background: The recently released WHO2019 classification of neuroendocrine neoplasm (NEN) of the digestive system includes a neuroendocrine tumor (NET) G3 category. An equivalent tumor group has also been recognized and studied in the lung. However, the clinicopathological and diagnostic features of NETs G3, especially in the lung, need to be improved.

Design: We reviewed 1425 NENs from various organs regarding prevalence, primary site, metastatic incidence and immunohistochemical characteristics of NETs G3.

Results: The case cohort included 1001 (70%) NETs, 222 (16%) neuroendocrine carcinomas (NECs) and 202 (14%) mixed non-neuroendocrine neuroendocrine neoplasms. 114 (8%) NENs were diagnosed as NET G3. The most frequent primary site of NET G3 was the pancreas (N=45, 39%), followed by lung (N=15, 13%), and stomach (N=10, 9%). NET G3 were rare in small intestine (4%), colon (3%), rectum (2%), duodenum (1%), and esophagogastric junction (1%), and absent in the appendix. Eighty-one percent of NET G3 patients had already metastases at the time of diagnosis, while patients with NET G1/G2 and NEC had metastases in only 38% and 79%, respectively ($p<0.0001$). Immunohistochemically, islet 1 labelled all metastatic pancreatic NETs G3 (100%), but none of the metastatic lung NETs G3 (0%, $p<0.0001$). In contrast, TTF1 was expressed in 70% of metastatic lung NETs G3, but not in metastatic pancreatic NETs G3 (0%, $p=0.002$). Insulin, glucagon, pancreatic-polypeptide, and somatostatin were positive in 60%, 22%, 17% and 14% of metastatic pancreatic NET G3, respectively. Metastatic lung NETs G3 were positive for serotonin (80%), and calcitonin (67%) and for somatostatin and gastrin related peptide in a few cases. The site of tumor origin remained unknown in 23% of NET G3, even if clinical history and immunohistochemistry were combined. This was a significantly higher rate than in NETs G1/G2 (8%), and was similarly high to the rate in NEC (27%, $p<0.0001$).

Conclusions: NET G3 arises from a broad variety of organs with a certain propensity in the gastrointestinal tract and lung. NET G3 is a highly aggressive neoplasm, often with liver metastasis at the time of diagnosis. Morphological and immunohistochemical features of metastatic NET G3 usually maintain the organotypic features of the primary tumor.

583 Application of PASS/GAPP Scores and Immunohistochemical Analysis of Pheochromocytoma/Paraganglioma (PHEO/PGL)

Beyza Keskin[1], Pelin Bagci[2], Emine Bozkurtlar[2], Handan Kaya[2]
[1]Istanbul, Pendik, Turkey, [2]Marmara University, Istanbul, Turkey

Disclosures: Beyza Keskin: None; Pelin Bagci: None; Emine Bozkurtlar: None; Handan Kaya: None

Background: We aimed to revise our pheochromocytoma (PHEO)/ paraganglioma (PGL) cases, score them according to both Pheochromocytoma of the Adrenal Scaled Score (PASS) and Grading System for Adrenal Pheochromocytoma and Paraganglioma (GAPP) scoring systems, and analyse immunoexpression of SDH-B and ATRX.

Design: Slides of PHEO/PGLs between 2012-19 were re-scored with new immunohistochemical markers, and compared with prognostic parameters.

Results: N=44, 13 PGL, 29 PHEO, and 2 had both PHEO and PGL. F/M: 27/17. Mean age: 47 (15-74). Tumor locations were: 9 intraabdominal, 6 neck, 29 adrenal. Mean diameter of the tumor was 5.7 cm. Thirteen had hypertension attacks and 1 had intracranial hemorrhage. The majority of the others diagnosed incidentally. Two had VHL syndrome, 1 *VHL* gene positivity, 1 medullary thyroid carcinoma and *RET* oncogene positivity. Two had a family history of VHL syndrome, and 2 had a family history of PHEO. PASS scores <4 in 16 (benign behavior), and GAPP ≤2 in 16 (well differentiated), 3-6≤ in 27(moderately differentiated).

Six cases demonstrated loss of SDH-B (Figure 1). All were negative for P53, Ki67 ≤ 1,5%. PASS scores <4 in 2. GAPP ≤2 in 1, 3-6≤ in 5. The mean diameter found to be 5,6 cm. One had a family history of PHEO, and *VHL* gene was positive in only one case. ATRX was positive in all.

Fourty one had strong cytoplasmic positivity with ATRX (Figure 2). No nuclear staining was observed in any of the cases.

Figure 1 - 583

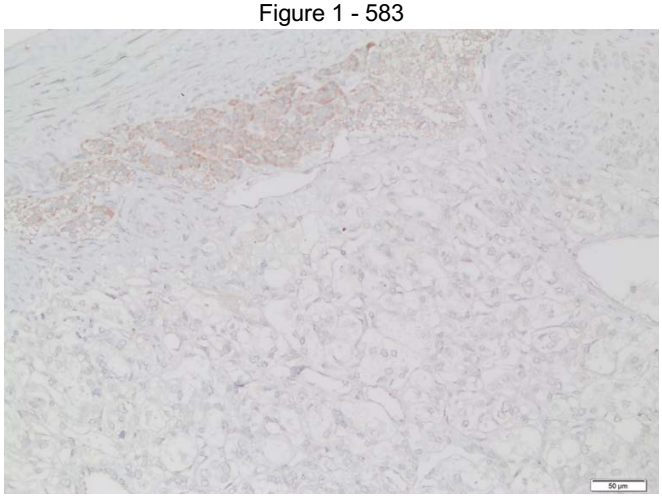

Figure 2 - 583

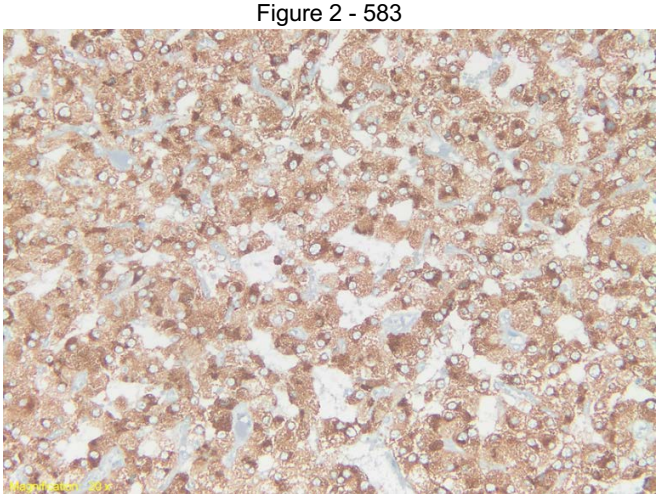

Conclusions: SDH-B staining loss was seen in 13,6% of the cases. One had *VHL* gene positivity. This shows SDH-B mutation can be seen in patients with *VHL* syndrome. We could not reveal any correlation between GAPP and PASS scores and SDH-B loss.

ATRX nuclear loss is a prognostic parameter in neuroendocrine tumors. None of our cases had nuclear staining, but they all demonstrated diffuse cytoplasmic staining. Cytoplasmic expression was seen in the adjacent adrenal medulla too, which could be related to the clone that we used (D-5, SC-55584).

584 The Histopathologic Check Points for Thyroid Core Needle Biopsy Comparative with Resection Sections and a Recommendation for Diagnostic Algorithm

Tugce Kiran[1], Beril Guler[1]
[1]*Istanbul, Fatih, Turkey*

Disclosures: Tugce Kiran: None; Beril Guler: None

Background: The Core-needle biopsy (CNB) method is gradually becoming more popular in the evaluation of thyroid nodules. However, the fact that nuclear features that are thought to be classic signs are not fully observed in these biopsy sections is an important diagnostic handicap. This issue has attracted limited attention in current studies. The aim of this study was to evaluate the histopathological differences between CNB samples and resection sections.

Design: The Hematoxylin and Eosin stained CNB and resection sections of thyroid nodules were reevaluated together in terms of nuclear and architectural parameters retrospectively. The evaluation was conducted by two pathologists. Statistical analysis was applied in 80 selected cases diagnosed as benign(n:37) and papillary carcinoma/suspicious for papillary carcinoma(n:43). Nuclear features (nuclear enlargement/irregularity, hypo/hyperchromia, clearing, groove, pseudoinclusion and overlapping) were grouped according to existence. Architectural findings were excluded from statistical evaluation.

Results: Colloid-containing follicular structures of various diameters were observed in benign lesions. A follicular and classic papillary pattern was dominant in malignant lesions. Trabecular, solid and Warthin-like architectures were the other structural features we noted. In the medullary carcinoma cases, oncocytic features were observed in one case in addition to the classic spindle morphology. The nuclear findings were more subtle than in resection sections. The nuclei were smaller (measurements of nuclear area, major axis and minor axis in CNB and resection sections were 52.62μm^2, 9.89μm, 6.75μm and 129.18μm^2, 14.53μm, 10.79μm respectively) (Figure 2). Nuclear clearing was not observed in any cases. Hypochromia was detected 46.5 % of papillary carcinoma cases. Grooves and pseudoinclusions were the other nuclear features that could be observed. However, nuclear contour irregularity was the most reliable finding that could predict papillary carcinoma diagnosis for CNB sections (v:0.82, p<0,001).

Diagnostic algorithm suggestion (Figure 1).

Figure 1 - 584

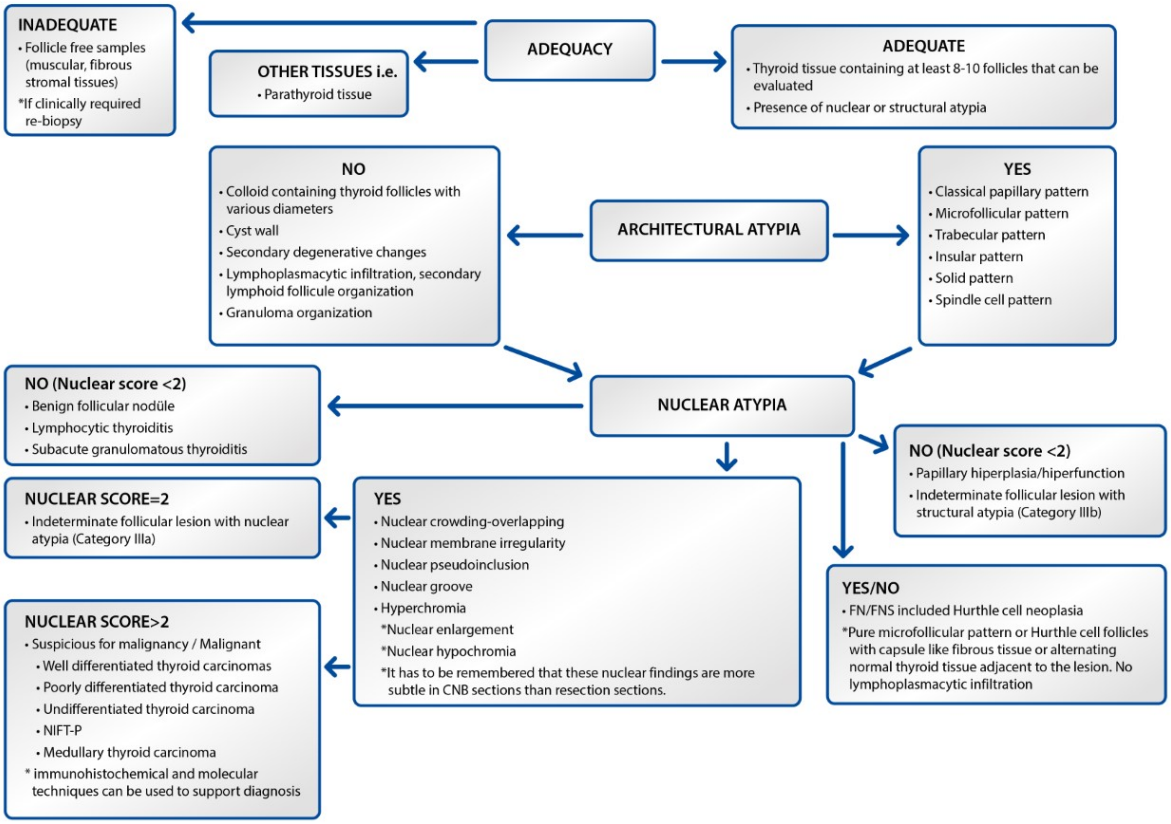

Figure 2 - 584

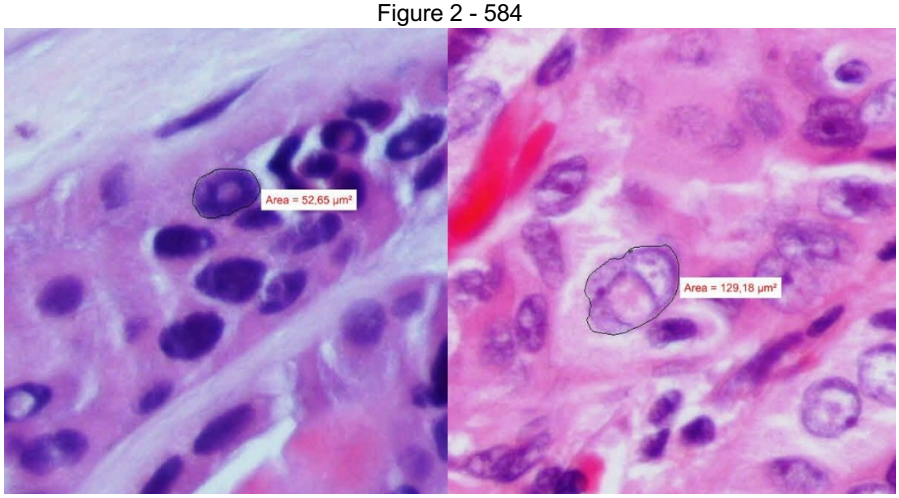

Conclusions: The CNB method is becoming more popular although its role in the approach to thyroid lesions is still controversial. We believe the histopathological differences that are not sufficiently covered in the literature but have an important diagnostic place should be emphasized and new diagnostic algorithms should be developed. We wanted to share the morphological features we observed at our center where CNB is used as the first step procedure.

585 Evaluating Cytological, Ultrasound and Molecular Features of Indeterminate Thyroid Nodules

Amanda Kornfield[1], Sam Sirotnikov[1], Deborah Baumgarten[1], Joshua Kagan[2], Melinda Lewis[1], Qiuying (Judy) Shi[3]
[1]Emory School of Medicine, Atlanta, GA, [2]Emory University, Decatur, GA, [3]Emory University, Atlanta, GA

Disclosures: Amanda Kornfield: None; Sam Sirotnikov: None; Deborah Baumgarten: None; Joshua Kagan: None; Melinda Lewis: None; Qiuying (Judy) Shi: None

Background: As indeterminate thyroid nodules on cytology fine needle aspirates (FNAs) are frequently encountered, determination of cancer risk of a particular nodule is crucial. Advances in risk determination have improved substantially with both expansion of genetic alterations detected on ThyroSeq v3 (Tv3) molecular testing and improved specificity of ultrasound. The 2015 American Thyroid Association (ATA) ultrasound guidelines can be correlated with molecular results to determine overall cancer risk.

Design: Data inquiry for 49 indeterminate thyroid nodules - 29 atypical undetermined significance (AUS, Bethesda III), 14 suspicious for follicular nodule (SFN, IV) and 6 suspicious for malignancy/PTC (SM, V) from 2017-2019. Patients with BRAF, RAS-related mutations and other mutations on Tv3 testing were selected. Additional follow-up for thyroidectomy and final histologic diagnosis was sought. Nodules were stratified on ultrasound according to ATA classification into very low, low, intermediate and high risk. Final histologic diagnosis was subclassified into carcinoma, noninvasive follicular thyroid neoplasm with papillary-like nuclear features (NIFTP) or benign. Based on the ultrasound risk stratification and final histologic diagnosis, cytology-histology-ultrasound-molecular correlation was determined.

Results: The data of 49 patients with indeterminate nodules was analyzed. The average age was 50.8 (range of 25-83). The male:female was 11:38. Nodules ranged in size from 0.6-6.8 cm (median size of 2.8 cm) and right:left:isthmus ratio of 26:21:2. 7 patients had BRAF, 33 patients had RAS - related mutations (HRAS, NRAS, KRAS, PAX8/PPARG, DICER1, THADA, PTEN or EIF1AX), 4 had other (NIS, CNA) alterations and 5 had no mutation. 53% (26/49) had cancer: 26.9% of BRAF mutations, 73% of RAS related mutations, 3.8% of other alterations, and 3.8% of cases without a mutation. 12.1 % of RAS related mutations had a final histologic diagnosis of NIFTP. By ATA classification, 78.8% of RAS related mutations were classified as very low, low, or low-intermediate (low-int). In BRAF mutation cases, 42.9% of cases were classified as very low, low, or low-int [see table attached].

Mutations from ThyroSeq v3 correlated with Bethesda class, histology and ultrasound findings

Tv3 Mutation Detected	Cytology (Bethesda Category)	Histology	Radiology (ATA classification)
BRAF (7)	III 1 IV 3 V 3	PTC 5 No Surgery 2	Very low 1 Low 1 Low-int 1 High 2 No category 2
RAS related (33) NRAS (15) HRAS (8) KRAS (3) Other RAS (7)	III 23 IV 7 V 3	FC 4 HC 2 FVPTC 7 PTC 6 NIFTP 4 Benign 9 No Surgery 1	Very low 1 Low 21 Low-int 4 Int 5 High 1 No images 1
NIS(2) CNA (2)	III 2 IV 2	FC 1 Benign 3	Low 1 Int 3
None (5)	III 3 IV 2	FVPTC 1 Benign 3 No Surgery 1	Very low 1 Low 2 Low-int 1 Int 2

PTC: Papillary Thyroid Carcinoma, FC=Follicular Carcinoma, FVPTC=Follicular variant papillary thyroid carcinoma, HC = Hurthle cell carcinoma

Conclusions: Indeterminate thyroid nodules can be difficult to distinguish on cytology specimens. Risk stratification based on ultrasound classification also shows overlapping features. Combining molecular testing with cytology and ultrasound features is essential to determine cancer risk prior to optimizing therapeutic options.

586 Retinoblastoma Co-repressor 1 (RB) and Cyclin-Dependent Kinase Inhibitor (CDKN) as a Two Gene Panel for Differentiating Pulmonary from Non-Pulmonary Origin in Metastatic Neuroendocrine Carcinomas

Kritika Krishnamurthy[1], Vathany Sriganeshan[1], Robert Poppiti[2]
[1]Mount Sinai Medical Center, Miami Beach, FL, [2]Mount Sinai Hospital, Miami Beach, FL

Disclosures: Kritika Krishnamurthy: None; Vathany Sriganeshan: None; Robert Poppiti: None

Background: Neuroendocrine carcinomas (NECs) often present with metastases even with small and undetectable primary tumors. NECs arise from neuroendocrine cells present throughout the body, with lung and GI tract being the most common primary sites. Additionally, neuroendocrine differentiation can be seen in undifferentiated carcinomas of non-neuroendocrine origin further complicating the landscape of metastatic NECs. Organ specific immunohistochemical markers such as TTF1, CDX2 and PAX8 are often lost in high grade tumors and may be non-contributory in localizing the primary site.

Thus in patients presenting with metastatic NEC, identifying the primary tumor can be challenging. Though NECs share a common cellular origin, they exhibit great variability in biologic behavior, prognosis and treatment based on the primary organ of origin.

Design: Twenty one cases of metastatic NECs were retrieved from our archives and were classified based on location of the primary tumor derived from clinical and radiological findings. Next generation sequencing data was retrieved and analyzed for recurrent genetic abnormalities in these cases. Statistical analysis was performed using IBM SPSS25 software.

Results: Genetic alterations were found in 128 genes in the 21 cases studied

RB1 mutations were exclusive to NECs metastasizing from lung primary and were detected in 5 of 12 (41.6%) cases (p=0.04). The RB1 mutation frequency did not vary significantly between small cell or large cell NEC of the lung.

CDKN gene family (CDKN1B and 2 A) mutations were limited to metastatic NECs of non-pulmonary origin and were detected in 4 of 9 (44.4%) cases (p=0.02).

Conclusions: The location of the primary tumor in metastatic NECs appears to have significant prognostic and therapeutic implications. But due to the morphological homogeneity, higher grade of tumor, variable sensitivity of immunohistochemical markers, and small, often undetectable primary tumors, the localization of the primary tumor in cases of metastatic NECs is a challenge. In this scenario, the detection of molecular variations specific to organ of origin may aid in establishing the location of the primary tumor and effect its further management. In this study, RB1 and CDKN gene family mutations are identified as possible markers for differentiating pulmonary and non-pulmonary origin in metastatic NECs.

587 MiNENs Composed of Adenocarcinoma and Well Differentiated Neuroendocrine Tumor Have a Monoclonal Origin

Stefano La Rosa[1], Michele Simbolo[2], Claudio Luchini[3], Albarello Luca[4], Jean-Yves Scoazec[5], Marco Schiavo Lena[6], Fausto Sessa[7], Aldo Scarpa[8]
[1]CHUV, Lausanne, VD, Switzerland, [2]University of Verona, Verona, VR, Italy, [3]University of Verona, Verona, Italy, [4]San Raffaele Hospital, Milano, Italy, [5]Gustave Roussy, Cancer Campus, Grand Paris, Villejuif, France, [6]San Raffaele Hospital, Milan, Italy, [7]University of Insubria, Varese, Italy, [8]Università di Verona, Verona, Italy

Disclosures: Stefano La Rosa: None; Michele Simbolo: None; Claudio Luchini: None; Albarello Luca: None; Jean-Yves Scoazec: None; Marco Schiavo Lena: None; Fausto Sessa: None; Aldo Scarpa: None

Background: MiNEN composed of adenocarcinoma (Ad) and well differentiated neuroendocrine tumor (NET) are rare and their molecular profile is unknown.

Design: Six MiNENs composed of Ad and NET were evaluated. Mutational and Copy Number Variation analysis was performed using the next-generation sequencing Oncomine Tumor Mutational Load assay (ThermoFisher) on DNA from FFPE tissues of microdissected MiNEN components.

Results: Four patients were females and two males (average age, 60 years). One MiNEN was located in the ampulla of Vater and 5 in the rectum. The NET component was G1 in 3 cases, G2 in 2 cases, and G3 in 1 case. In each tumor, the Ad and NET components presented the same molecular alterations. A total of 38 mutations in 12 genes were identified, including 24 missense, 6 nonsense, 2 frameshift and 6 splice site alterations. Mutations in *TP53* gene were found in 4 cases, in *KRAS* in 3, in *HRAS* in 1, and in *APC* in 2. Among genes involved in chromatin remodeling, mutations were detected in *SMARCA4* in 1 case and in *ARID1A* in another one. Among genes involved in the mTOR pathway, *AKT1* and *MTOR* mutations were observed in 1 case and *PIK3CA* in another. Homozygous deletions of *CDKN2A/B* were

detected in 4 cases; focal low copy gains (3-4 copies) of *CCNE1* and *BCL2L1* were found in 2 cases. Chromosome 18 LOH was found in 4 cases. Four patients were alive free of disease after a mean follow-up time of 11 months (range 9-13 months), one was alive with disease after 57 months and one died of disease after 36 months.

Conclusions: MiNENs composed of Ad and NET are less aggressive than MiNENs composed of Ad and NEC (MANEC). Our molecular analysis demonstrates for the first time that the two components (Ad and NET) present the same molecular alterations in each tumor suggesting a monoclonal origin from a common precursor progenitor cell.

588 Detection of NTRK1/3 Rearrangements in Papillary Thyroid Carcinoma Using Immunohistochemistry and Fluorescent in Situ Hybridization

Yu-Cheng Lee[1], Jen-Fan Hang[2]
[1]Taipei Veterans General Hospital, Yonghe District, New Taipei City, Taiwan, [2]Taipei Veterans General Hospital, Taipei, Taiwan

Disclosures: Yu-Cheng Lee: None; Jen-Fan Hang: None

Background: Papillary thyroid carcinoma (PTC) is the most common malignancy of the thyroid gland and the majority harbors BRAF V600E mutation. NTRK1/3 rearrangements have been reported in up to 5.2% of PTC and are regarded as potential therapeutic targets of the newly available TRK inhibitors. Recently, the application of immunohistochemistry (IHC) using pan-TRK antibody to detect NTRK gene fusions has been widely discussed in lung, colon, breast, and salivary gland cancers. However, the validation data in PTC is lacking. The study aimed to examine the sensitivity and specificity of pan-TRK IHC for detecting NTRK1/3 gene rearrangements in PTC and to compare IHC with fluorescent in situ hybridization (FISH).

Design: A retrospective review of PTC cases from surgical pathology archives between October 2015 and March 2019 with available BRAF mutation status was performed. Cases with tumor size smaller than 0.5 cm or with features consistent with noninvasive follicular thyroid neoplasm with papillary-like nuclear features (NIFTP) were excluded. Formalin-fixed paraffin-embedded (FFPE) tissues of BRAF-negative, non-cribriform-morular variant (CMV) of PTC were subject to tissue microarray (TMA) construction. Pan-TRK IHC (clone EPR17341, Abcam, Cambridge, MA) and NTRK1, NTRK3, and ETV6 break-apart FISH (ZytoVision, Bremerhaven, Germany) were performed.

Results: A total of 526 consecutive PTC cases, including 456 (86.7%) BRAF-positive PTC and 70 (13.3%) BRAF-negative PTC, were identified. Excluding 4 cases of CMV of PTC and 5 cases with suboptimal tissues for FISH, there were 61 BRAF-negative PTC which underwent complete evaluation of IHC and FISH. Twelve cases were positive by FISH, including 6 cases with ETV6-NTRK3 rearrangement, 4 with X-NTRK3 rearrangement, and 2 with X-NTRK1 rearrangement. Pan-TRK IHC was positive in 1 case with ETV6-NTRK3 rearrangement (16.7%, 1/6), 2 with X-NTRK3 rearrangement (50%, 2/4), 2 with X-NTRK1 rearrangement (100%, 2/2), and was negative in all FISH-negative cases. As a result, pan-TRK IHC showed a sensitivity of 41.7% (5/12) and specificity of 100% for detecting NTRK1/3 rearrangements in BRAF-negative PTC.

Conclusions: Pan-TRK IHC was highly specific for detecting NTRK1/3 rearrangements in PTC. The sensitivity was high for NTRK1-rearranged PTC but low for NTRK3-rearranged PTC. Based on the results, utilizing pan-TRK IHC and followed by NTRK3 FISH in IHC-negative cases would be a reasonable strategy for detecting NTRK1/3 rearrangements in PTC.

589 Pheochromocytoma: Clinicopathological and Molecular Study of 333 Cases

Zhonghua Liu[1], Camilo Jimenez[2], Miao Zhang[3]
[1]The University of Texas MD Anderson Cancer Center, Austin, TX, [2]The University of Texas MD Anderson Cancer Center, Houston, TX, [3]The University of Texas MD Anderson Cancer Center, Bellaire, TX

Disclosures: Zhonghua Liu: None; Camilo Jimenez: None; Miao Zhang: None

Background: Pheochromocytomas (PHEO) are rare tumors. The prevalence of the newly discovered clinically relevant molecular signatures, such as SDHB mutation, is unknown. Herein, we evaluate a large cohort of PHEO to address the prevalence and molecular characteristics to help predict behavior.

Design: We retrospectively reviewed cases of PHEO from the institution archives from 1956 to 2014. These cases were analyzed for clinical presentation, family history, location, size, mutation status and overall survival.

Results: 333 cases (M: F=154:179) with the mean age at diagnosis of 43.4 yrs (6-83yrs) were identified. 15 patients (4.5%) were younger than 18 yrs. 18.6% (n=62) had a family history of PHEO. 12.6% (n=42) were asymptomatic and found incidentally by imaging study. 73% (n=243) were non-metastatic. 27% (n=90) were with metastasis. The mean tumor size was 5.3 cm (0.7-21 cm) in non-metastatic cases and 9.9 cm (2.2-28 cm) in metastatic cases. 60 cases involved bilateral adrenal glands and they were all non-metastatic cases. 41.4% of cases (n=138, 125 non-metastatic and 13 metastatic) were associated with a hereditary syndrome including MEN1, MEN2A, MEN2B, VHL, NF1,

familial paraganglioma syndromes (PGL) types 1 and 4. 144 patients underwent molecular testing. Mutations in *RET*, *SDHB*, *SDHD*, *VHL*, and *NF1* genes were identified (Table 1). All 8 cases with *SDHB* mutation were metastatic, while 5 cases of *SDHD* mutation were non-metastatic. 112 patients died at the end of study, 22.6% (n=55) were non-metastatic and 63.3% (n=57) were metastatic, with 5-year overall survival rate of 94.7% and 72.2% respectively (P<0.01).

Table 1. Molecular and genetic status in 333 cases of pheochromocytoma.

		Non-metastatic pheochromocytoma	Metastatic pheochromocytoma
Hereditary syndrome	MEN1	2	0
	MEN2A	71	1
	MEN2B	14	0
	PGL1	5	0
	PGL4	1	8
	VHL	23	2
	NF1	9	2
Gene mutation	*RET*	55	2
	SDHB	0	8
	SDHD	5	0
	VHL	15	2
	NF1	1	0

Conclusions: Our data showed that 27% of cases of PHEO were metastatic with unilateral involvement, larger tumor size, and shorter overall survival. 41.4% of cases occurred in the context of inherited syndromes. Among these patients, the associated PHEO were mostly non-metastatic. Mutations in *RET*, *VHL* and *SDHD* genes were more commonly observed in non-metastatic cases; however, *SDHB* mutation showed strong association with metastatic cases. Our data suggests that all patients with PHEO should undergo molecular testing and *SDHB* gene mutation has a strong prognostic value.

590 Adrenal Cystic Lesions of Lymphatic Origin: A Clinical and Pathological Study of 6 New Cases and Systematic Literature Review

Mario Marques-Piubelli[1], Eloiza Poma-Gonzalez[2], Marcelo Balancin[3], Victor Gonçalves[2], Maria Luiza Botelho[4], Maria Fragoso[5], Maria Zerbini[6]

[1]The University of Texas MD Anderson Cancer Center, Houston, TX, [2]Hospital das Clínicas da Faculdade de Medicina da USP, São Paulo, SP, Brazil, [3]University of São Paulo, São Paulo, SP, Brazil, [4]Rede D'OR - São Luiz, São Paulo, SP, Brazil, [5]Faculdade de Medicina FMUSP, São Paulo, SP, Brazil, [6]Faculdade de Medicina da USP, São Paulo, SP, Brazil

Disclosures: Mario Marques-Piubelli: None; Eloiza Poma-Gonzalez: None; Marcelo Balancin: None; Victor Gonçalves: None; Maria Luiza Botelho: None; Maria Fragoso: None; Maria Zerbini: None

Background: Cystic lesions of the adrenal gland are rare lesions and usually incidentally discovered. These lesions are categorized into four major histopathologic groups: endothelial cysts, pseudocysts, epithelial cysts, and parasitic cysts. Endothelial cysts are 45% of all adrenal cysts and the most common subtypes include adrenal cyst of lymphangiomatous origin (ACLO) and adrenal lymphangioma (AL).

Design: We retrospectively analyzed our ten-year experience regarding the histopathological diagnostic of adrenal cysts and performed a systematic literature review about ACLO and AL from 1965 to June/2019, including two external cases (cases 13, 14).

Results: Case series: of the 14 selected cases, we found four ACLO (31%), one AL (7%), three pseudocysts (23%), three epithelial cysts (23%), one epithelial cyst of thyroid ectopic tissue in adrenal cortex (8%), and one adenomatoid tumor of adrenal gland (8%). Other macroscopic and immunohistochemistry features of the cysts are summarized in Table 1. Regarding our ACLO and AL cases (n = 6), four patients were female and 2 male. Five patients were of Caucasian ethnicity and the mean age were 35 years, ranging from 27 to 44 years. Four lesions were in the right adrenal and two in the left. The mean size of 6.4 cm. One case had another cystic lesion associated with the ipsilateral kidney. Figure 1 and 2 show the histopathological and immunohistochemical features of AL and ACLO.

Literature review: we found 108 cases of ACLO and AL from 57 articles. The sex distribution was 2.2F:1M and had discrete predominance in the right adrenal. CD31 was positive in 50/51 cases, CD34 was positive in 21/29 cases and D2-40 was positive in 53/53 cases. Pancytokeratin AE-1/AE-3 was negative in all twenty-four tested cases and Factor VIII was positive in six of eight cases. Only one series performed ERG and were positive in all eight cases of AL. Fifteen of 53 cases had secretion of catecholamines during the diagnostic workup. All cases had surgical treatment, and the majority of them underwent to open adrenalectomy (59/93).

Case Number	Sex/Age (years)	Adrenal laterality	Adrenal Weight	Macroscopic size (Lesion)	Cyst Wall (color)	Cyst Inner surface	Cyst Loculation	CD 31	CD 34	AE-1/AE-3	Factor VIII	D2-402	ERG	WT-1	Other Antibodies	Hormone Secreting	Diagnostic
1	F/43	Right	NA	16.0 x 14.5 x 5.5 cm	Brownish and bloody	Smooth	Multiloculated	Positive	Negative	Negative	Positive	Positive	Positive	NA	No	No	Lymphangioma
2	F/27	Right	29.1 gr	4.0 x 4.0 x 2.5 cm	Brownish and white	Smooth	Multiloculated	Positive	Positive	Negative	Negative	Positive	Positive	NA	No	NA	Endothelial Cyst (Lymphangiomatous type)
3	F/53	Left	132.3 gr	5.5 x 4.0 x 3.5 cm	Brownish	Irregular with multiple calcificated areas	Multiloculated	Negative	Negative	Negative	Negative	Negative	Negative	NA	No	Urinary Vanillymandelic acid (24 hrs): 26 mg/24 hrs (nl: 2.0 - 12.0 mg/24 hrs)	Pseudocyst
4	F/73	Right	60 gr	3.7 x 3.7 x 3.7 cm	NA	NA	Uniloculated	Negative	Negative	Positive	Negative	Negative	Negative	Positive	No	No	Epithelial cyst
5	F/49	Left	8.2 gr	2.0 x 1.1 x 0.8 cm	Brownish	Smooth	Uniloculated	Negative	Negative	Negative	Negative	Negative	Negative	NA	No	No	Pseudocyst
6	M/36	Right	25.7 gr	5.0 x 5.0 x 1.3 cm	Brownish	Smooth	Uniloculated	Positive	Negative	Negative	Positive	Positive	Positive	NA	No	No	Endothelial Cyst (Lymphangiomatous type)
7	F/55	Right	21.1 gr	4.3 x 4.3 x 4.3 cm	White	Smooth	Uniloculated	Negative	Negative	Positive	NR	Negative	Negative	Positive	No	No	Epithelial cyst
8	F/38	Right	NA	3.5 x 3.0 x 3.0 cm	White	Smooth	Uniloculated	Positive	Negative	Negative	Positive	Positive	Positive	NA	No	NA	Endothelial Cyst (Lymphangiomatous type)
9	F/57	Left	19.2 gr	2.5 x 2.5 x 2.3 cm	Brownish	Smooth	Uniloculated	Negative	Negative	Negative	Negative	Negative	Negative	NA	No	Norepinephrine: 287 pg/ml (nl: 40.0 - 268.0 pg/ml)	Pseudocyst
10	F/72	Right	38.8 gr	8.0 x 7.2 x 1.2 cm	Gray	Smooth	Uniloculated	Negative	Negative	Positive	Negative	Negative	Negative	Positive	No	Norepinephrine: 429	Epithelial cyst

																pg/ml (nl: 40.0 - 268.0 pg/ml)	
11	F/43	Left	144.1 gr	5.3 x 2.1 x 4.0 cm	Gray	Smooth	Unilocculated	Negative	Negative	Positive	Negative	Negative	Positive	NA	Thyroglobulin and TTF1 positive	No	Epithelial Cyst with origin in thyroidian ectopic tissue of adrenal cortex
12	M/44	Left	65.2 gr	5.5 x 2.5 x 1.0 cm	Gray	Smooth	Unilocculated	Positive	Negative	Negative	Positive	Positive	Positive	NA	No	No	Endothelial Cyst (Lymphangiomatous type)
13	M/40	Right	62,4 gr	5,0 x 4,7 x 2,8 cm	White	NA	Multiloculated	Negative	Negative	Positive	NR	Positive	NR	Positive	No	NA	Adenomatoid tumor
14	F/28	Left	10.6 gr	4.5 x 2.7 x 1.5 cm	Gray	Smooth	Unilocculated	Positive	Negative	Negative	NA	Positive	Positive	NA	Calretinin and Melan A negative	NA	Endothelial Cyst (Lymphangiomatous type)
NA: not available																	

Figure 1 - 590

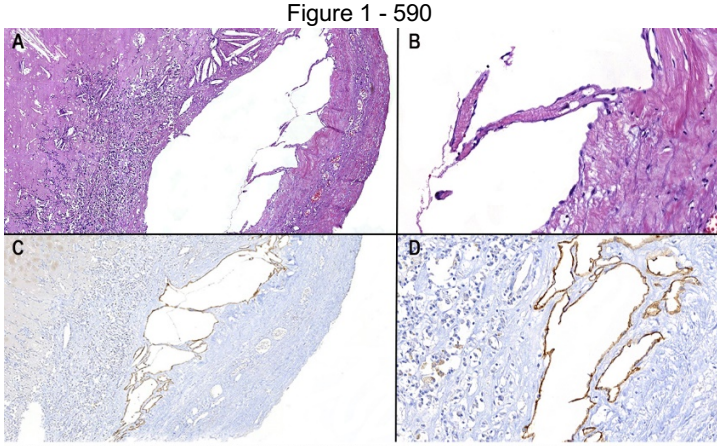

Figure 1. A) Hematoxylin & Eosin section showing a multiloculated appearance and cyst content (50x); B) Hematoxylin & Eosin sec a cystic space lined by a single layer of flattened cells; C and D) The flat lining cells showing strongly positivity for D2-40 stain (im chemistry, 50 and 200x).

Figure 2 - 590

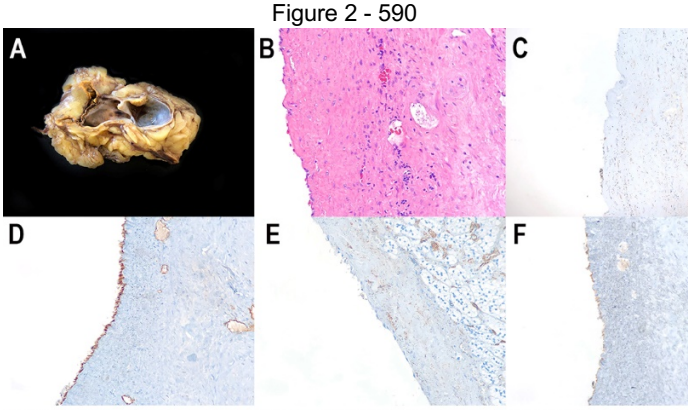

Figure 2. Histopathological and immunohistochemistry profile of Adrenal Lymphangiomas: A) Macroscopic app a multiloculated adrenal lymphangioma; B) Hematoxylin & eosin section showing a single lining the internal cys (200x); C) Pancytokeratin (AE-1/AE-3) negativity in immunohistochemistry (200x); D) D2-40 positivity in immun mistry (200x); E) CD31 negativity in immunohistochemistry (200x); F) ERG positivity in immunohistochemistr

Conclusions: AL is a rare and benign lesion with no clear pathogenesis. It should be included in the differential diagnosis of adrenal and retroperitoneal lesions. The diagnostic is challenging and there is an important overlapping between the definition of adrenal cystic lymphangiomatous lesions and adrenal lymphangiomas. Surgical treatment and histopathological approach are necessary for both conditions to a correct diagnosis and follow-up.

591 Immunohistochemical Evaluation of Insulinoma-Associated Protein 1 (INSM1) Expression on Tumors and Normal Tissues from Various Organs

Mohammad Mohammad[1], Haiyan Liu[2], Jianhui Shi[2], Fan Lin[2]
[1]Geisinger Commonwealth School of Medicine, Danville, PA, [2]Geisinger Medical Center, Danville, PA

Disclosures: Mohammad Mohammad: None; Haiyan Liu: None; Jianhui Shi: None; Fan Lin: None

Background: Recent studies demonstrated that insulinoma-associated protein 1 (INSM1), a transcription factor, was a highly sensitive marker for diagnosing neuroendocrine tumors (NETs)/carcinomas (CAs) from various organs with the diagnostic sensitivity of approaching 100%. However, available data on INSM1 expression in non-neuroendocrine tumors are limited. In this study, we focused on the evaluation of INSM1 expression in a large series of non-neuroendocrine CAs and tumors from various organs.

Design: Immunohistochemical analysis of INSM1 (sc-271408; Santa Cruz Biotechnology) was performed on 1247 cases of tumor and normal tissues on tissue microarray (TMA) sections, including mesothelioma (N=18), lung neuroendocrine CA (N=24), lung adenocarcinoma (ADC) (N=88), lung squamous cell CA (N=66), papillary thyroid CA (N=47), ENT squamous cell CA (N=28), breast fibroadenoma (N=20), pancreatic NET (N=33), gastrointestinal (GI) NET (N=14), pancreatic ADC (N=43), adrenal pheochromocytoma (N=14), endometrial CA FIGO II (N=59), ovary papillary serous CA (N=41), clear cell CA of uterus and ovary (N=22), melanoma (N=32), skin neuroendocrine CA (N=27), invasive urothelial CA (N=43), bladder small cell CA (N=24), prostatic ADC (N=38), germ cell tumors (N=60), colonic ADC (N=164), angiosarcoma (N=12), papillary renal cell carcinoma (RCC) (N=33), clear cell RCC, low grade (N=79), clear cell RCC, high grade (N=51), hepatocellular CA (N=47), liver metastatic neuroendocrine CA (N=18), glioblastoma multiforme (GBM) (N=23), mantle cell lymphoma (N=13) and hairy cell leukemia (N=1). Samples from normal tissue included pancreas (N=13), rectum/appendix/colon (N=39) and ilium/duodenum/stomach (N=13). Nuclear expression for INSM1was interpreted as negative (<5% tumor cells stained), 1+ (<25%), 2+ (26-50%), 3+ (51-75%), and 4+ (>75%).

Results: The positive staining results are summarized in Table 1. With the exception of 1 NET from the lower GI tract and 8 of 24 (33%) small cell CAs of the bladder, all other NET/CAs were positive for INSM1. All other non-neuroendocrine tumors and normal tissues were negative. Representative cases are shown in Figure 1.

Table 1. Summary of the positive staining results

Diagnosis	Neg	1+	2+	3+	4+	Total positive cases (%)
Lung NET	0	2			22	24/24 (100%)
Pan NET	0	1	2		30	33/33 (100%)
Pheochromocytoma	0	1			13	14/14 (100%)
GI NET	1				13	13/14 (93%)
Skin NET	0	1	1		25	27/27 (100%)
Metastatic NET	0	2			16	18/18 (100%)
Bladder SCC	8				16	16/24 (67%)
GBM	21		2			2/23 (9%)
Melanoma	26		3	2	1	6/32 (19%)
Ovary serous CA	32	6		2	1	9/41 (22%)

Note: NET – neuroendocrine tumor/carcinoma; GI – gastrointestinal; SCC – small cell carcinoma

Figure 1 - 591

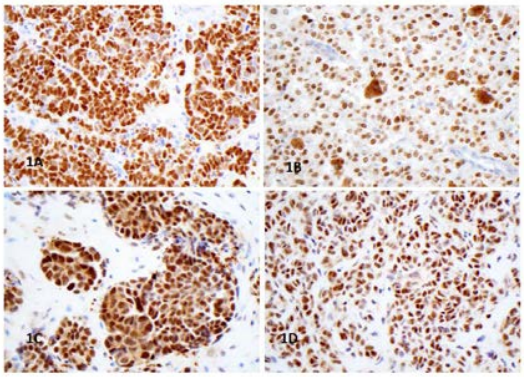

Figure 1 (1A through 1D) showing representative cases positive nuclear staining for INSM1.
Note that Merkel cell CA (1A), pheochromocytoma (1B), ovarian serous CA (1C), and melanoma (1D).

Conclusions: Our data demonstrated that INSM1is a highly sensitive and specific marker of neuroendocrine tumors. Caution should be taken because 1) a significant number of ovarian papillary serous CAs and melanoma can be positive for INSM1; and 2) SCC of the bladder can be negative for INSM1.

592 Long Noncoding RNA Expression in Pulmonary Neuroendocrine Carcinomas

Damodaran Narayanan[1], Ricardo Lloyd[2], Darya Buehler[3], Jason Rosenbaum[4], Michael Schwalbe[5], Heather Hardin[6], Vishal Chanana[7]

[1]University of Wisconsin Hospital and Clinics, Madison, WI, [2]University of Wisconsin, Madison, WI, [3]University of Wisconsin, Madison, Madison, WI, [4]UPenn, Center for Personalized Diagnostics, Philadelphia, PA, [5]Stanford University Medical Center, Palo Alto, CA, [6]University of Wisconsin-Madison, Madison, WI, [7]School of Medicine and Public Health, The University of Wisconsin-Madison, Madison, WI

Disclosures: Damodaran Narayanan: None; Ricardo Lloyd: None; Darya Buehler: None; Jason Rosenbaum: None; Michael Schwalbe: None; Heather Hardin: None; Vishal Chanana: None

Background: Long noncoding RNAs (lncRNAs) participate in transcription and in epigenetic or posttranscriptional regulation of gene expression; they also have a role in epithelial-to-mesenchymal transition and in carcinogenesis. Pulmonary neuroendocrine tumors (NETs) include low-grade indolent and high-grade aggressive carcinomas based on clinical behavior, histology, and possibly proliferation. This distinction is important for therapeutic choices and prognosis. LncRNAs may have a role in the development and progression of pulmonary NETs. We examined a group of pulmonary NETs to determine the role of specific lncRNAs in tumor development and progression.

Design: Three lncRNAs, including prostate cancer antigen 3 (*PCA3*), HOX transcript antisense RNA (*HOTAIR*), and Maternally Expressed 3 (*MEG3*), were used for *in situ* hybridization (ISH) analysis on a tissue microarray (TMA) and quantitative real-time polymerase chain reaction (qRT-PCR). The TMA consisted of 1 mm duplicate cores of typical carcinoid tumors (TC) (N=69), atypical carcinoid tumors (ATC) (N=18), and small cell carcinomas (SCC) (N=19). ISH was performed with RNAScope technology (Advanced Cell Diagnostics). The ISH images were analyzed with Vectra imaging technology and quantified using Nuance and inForm software. qRT-PCR was done using some of the same tissue blocks used for construction of the TMA. A cultured human small cell carcinoma cell line (H69) was used for *in vitro* studies with siRNA directed against the lncRNAs.

Results: ISH showed that expression of all three lncRNAs were significantly higher ($P<0.01$) in SCC compared to TC. In addition, expression of *PCA3* and *HOTAIR* in SCC was significantly higher than ATC. When comparing the ATC and TC groups, expression of *PCA3*, *MEG3*, and *HOTAIR* was significantly lower, significantly higher, and similar, respectively.

qRT-PCR showed higher expression of *PCA3* and *MEG3* in SCC compared to TC and ATC, but the elevated *MEG3* expression in SCC was not significant when compared to TC and ATC.

siRNA silencing of *PCA3* and *MEG3* resulted in inhibition of growth of the H69 cell line, supporting a role for these lncRNAs in tumor cell proliferation.

Conclusions: The lncRNAs *PCA3, HOTAIR*, and *MEG3* have regulatory roles in pulmonary NETs and may be important for tumor progression. Because these lncRNAs are highly expressed in higher grade NETs, they may serve as potential prognostic indicators of pulmonary NET aggressiveness and as possible therapeutic targets.

593 The Prognostic Value of Individual Parameters of the Weiss Scoring System in a Series of Adrenocortical Carcinomas

Gabriella Nesi[1], Letizia Canu[1], Raffaella Santi[2], Ilaria Galli[1], Giulia Cantini[1], Michaela Luconi[1]
[1]University of Florence, Florence, Italy, [2]Florence, Italy

Disclosures: Gabriella Nesi: None; Letizia Canu: None; Raffaella Santi: None; Ilaria Galli: None; Giulia Cantini: None; Michaela Luconi: None

Background: Adrenocortical carcinoma (ACC) is an uncommon tumor with variable prognosis. A number of studies have proposed histologic criteria to predict malignant behavior. Currently, the Weiss Score is the most widely used scoring system for diagnostic purposes, but it also possesses a prognostic value.

Design: The aim of our study was to assess the relative impact on survival of each Weiss parameter in a monocentric series of 38 ACC cases. The prognostic power of all nine individual morphologic criteria considered in the Weiss Scoring System was estimated by Kaplan-Meier analysis and compared to that of tumor stage, total Weiss score and Ki-67 labelling index.

Results: At Kaplan Meier analysis, tumor stage was the best predictor of Overall Survival (OS) (Log Rank p=0.000) and, among the Weiss parameters, necrosis showed a strong adverse impact (Log Rank p=0.014). As regards Disease-Free Survival (DFS), higher pathologic stage (Log Rank p=0.000), Ki-67 >10% (Log Rank p=0.017) and Weiss score >6 (Log Rank p=0.025) were all predictors of poor prognosis. Among the parameters of the Weiss Scoring System, both necrosis (Log Rank p=0.000) and capsular invasion strongly correlated with disease-free outcome status (Log Rank p=0.042). At regression analysis, a statistically significant positive association was found between necrosis, OS and recurrence (r=0.600, p=0.000 and r=0.396, p=0.015, respectively), while capsular invasion and Ki-67 were associated with recurrence (r=0.338, p=0.041 and r=0.415, p=0.0011, respectively) but not with OS.

Conclusions: Our report indicates necrosis as a relevant adverse factor and the best histologic predictor of OS, DFS and recurrence in patients with ACC.

594 Loss of 5-hydroxymethylcytosine is an Epigenetic Hallmark of Aggressive Thyroid Carcinomas

Naoki Oishi[1], Huy Vuong[1], Kunio Mochizuki[1], Tetsuo Kondo[1]
[1]University of Yamanashi, Chuo, Yamanashi, Japan

Disclosures: Naoki Oishi: None; Huy Vuong: None; Kunio Mochizuki: None; Tetsuo Kondo: None

Background: Epigenetic dysregulation is a hallmark of cancer. 5-hydroxymethylcytosine (5-hmC), a DNA hydroxymethylation at the 5 position of cytosine, is converted from 5-methylcytosine (5-mC) by the ten-eleven translocation (TET) family of DNA hydroxylases. Recent studies have shown that the global level of 5-hmC is significantly decreased in various cancers including melanoma and renal cell carcinoma, providing diagnostic and prognostic implications. However, 5-hmC dysregulation status has not been fully elucidated in thyroid carcinomas especially in association with *TERT* promoter mutation, an independent unfavorable prognostic factor.

Design: *BRAF* and *TERT* promoter status of papillary thyroid carcinomas (PTCs) and anaplastic thyroid carcinomas (ATCs) was examined by allele-specific PCR and/or Sanger sequencing. We evaluated global 5-hmC level by ELISA and/or immunohistochemistry (IHC) on normal thyroid (ELISA, n=5; IHC, n=8), *TERT*-wildtype PTCs (n=5; n=63), *TERT*-mutant PTCs (n=5; n=10), and ATCs (n=3; n=4). IHC was semi-quantified into 0 to 4 based on the %positive tumor cells: 0=0-1%; 1=1-10%; 2 = 10-25%; 3 = 25-75%; 4 = 75-100%.

Results: ELISA showed that 5-hmC level is significantly lower in *TERT*-mutated PTCs than in *TERT*-wildtype PTCs ($p<0.05$). No significant difference was observed between *TERT*-wildtype PTCs and normal thyroid tissues. 5-hmC IHC scores on selected samples well correlated with relative 5-hmC level measured by ELISA ($p<0.01$, $r^2=0.39$), validating the scoring system. Subsequent IHC further confirmed the lower 5-hmC in *TERT*-mutated PTCs and ATCs than that in normal thyroid tissues and *TERT*-wildtype PTCs (Figure 1A and 1B). Subgroups analysis on 73 PTCs showed that decreased 5-hmC level is associated with larger tumor size (>1cm), higher pathologic stage (stage II vs. I), and *TERT* promoter mutation, but not with patient's age, extrathyroidal invasion, lymph node metastasis, and *BRAF* mutation.

Figure 1 - 594

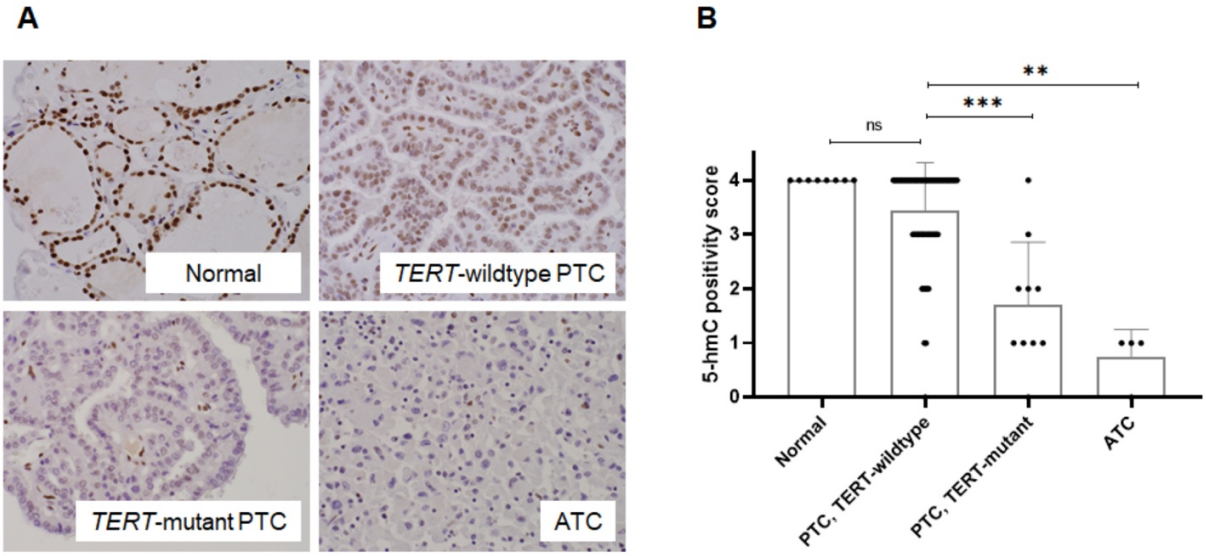

Conclusions: We, for the first time, elucidated that *TERT*-mutated PTCs and ATCs are characterized by loss of 5-hmC, further supporting distinct molecular biology of these aggressive thyroid carcinomas by distinct epigenetic dysregulation.

595 DICER1 Hotspot Mutations in Pediatric Thyroid Papillary Carcinoma: A Single Center Experience.

Semen Onder[1], Ismail Yilmaz[2], Aysel Bayram[3], Gizem Issin[4], Neslihan Kaya Terzi[5], Yalin İscan[6], Ismail Sormaz[6], Fatih Tunca[6], Yasemin Senyurek[6], Gulcin Yegen[7]

[1]Istanbul Medical Faculty, Istanbul, Turkey, [2]Istanbul Sultan Abdülhamid Han Education and Research Hospital, Department of Pathology, Istanbul, Turkey, [3]Department of Forensic Medicine, Ministry of Justice, Istanbul, Turkey, [4]Mengucek Gazi Education and Research Hospital, Erzincan Binali Yildirim university, Erzincan, Erzincan, Turkey, [5]Istanbul, Uskudar, Turkey, [6]Istanbul Faculty of Medicine, Istanbul University, Department of General Surgery, Istanbul, Turkey, [7]Istanbul Faculty of Medicine, Istanbul University, Istanbul, Turkey

Disclosures: Semen Onder: None; Ismail Yilmaz: None; Aysel Bayram: None; Gizem Issin: None; Neslihan Kaya Terzi: None; Yalin ?scan: None; Ismail Sormaz: None; Fatih Tunca: None; Yasemin Senyurek: None; Gulcin Yegen: None

Background: Pediatric papillary thyroid carcinoma (PPTC) is a distinct entity from its adult counterpart with its aggressive clinical behaviour and excellent prognosis. The discrepancy is maybe associated with different molecular profiles. DICER1 is a gene that plays a role in the miRNA processing and is found both at germline and somatic levels. Although DICER1 mutations are very rare in adult papillary thyroid carcinoma cases, it is accepted to be one of the driver events in thyroid carcinomas. The objective of this study is to investigate the prevalence and the prognostic impact of DICER1 hotspot mutations in PPTC.

Design: Fifty PPTC cases that were diagnosed between 1995 and 2015 were selected from pathology records of our pathology department. All cases were reviewed by endocrine pathologists and the diagnosis was confirmed according to current guidelines. Complete clinical follow-up information were also obtained. The representative formalin-fixed paraffin-embedded tumor samples were selected for DICER1 mutation analysis. Mutations in exon 26 and 27 of DICER1 gene (well-known hotspot regions for pathogenic mutations) were analyzed by PCR based direct sequencing.

Results: Among 50 patients, DICER1 hotspot mutations were detected in 7 patients (14%). The mutations were detected at four sites: E1705 (1/7), D1709 (2/7), G1810 (2/7) E1813 (2/7) (Figure 1) with a novel D1810del mutation. We confirmed that the mutations were somatic by using matched-normal DNA of the mutated cases. The histologic types of the mutant cases were classic variant (n=3), invasive follicular variant (n=2), microcarcinomas that were follicular variant (2). The median patient age was 16, ranging from 6 to 18. The duration of follow-up time was 118 months. Distant metastasis and local recurrence were detected in 5 (10%) and 7 (14%) of the patients, respectively. None of DICER1 mutant patients showed distant metastasis or local recurrence. Similarly lateral lymph node metastases were not detected in DICER1 mutant patients, whereas 16 (37%) of the other patients had showed (p=0.08). No significant difference was detected between PPTC with or without DICER1 mutations in survival analysis.

Figure 1 - 595


DICER1 Exon 27 Negative Control
DICER1 Exon 26 Negative Control
c.5429A>T (p.D1810V)
c.5113G>A (p.E1705K)
c.5437G>C (p.E1813Q)
c.5125G>A (p.D1709N)
c.5439G>T (p.E1813D)
c.5126A>G (p.D1709G)
c.5428_5430delGAT (p.D1810del)

Conclusions: DICER1 hotspot mutations are not infrequent in PPTC cases. The prognostic value of DICER1 mutations in PPTC is still under debate due to limited number of patients, like our cohort. More studies with large number of pediatric patients are needed to clarify the role of DICER1 hotspot mutations on prognosis and tumorigenesis.

596 Alpha-inhibin Expression in Paragangliomas and Pheochromocytomas Shows Strong Correlation with VHL- and SDHx-driven Pseudohypoxic Pathway Disease

Sara Pakbaz[1], Sylvia Asa[2], Ozgur Mete[3]
[1]University Health Network, Toronto, ON, [2]Case Western Reserve University/University Hospitals Cleveland Medical Center, Toronto, ON, [3]University Health Network, University of Toronto, Toronto, ON

Disclosures: Sara Pakbaz: None; Sylvia Asa: *Advisory Board Member*, Leica Biosystems Advanced Staining and Imaging Medical Advisory Board; *Advisory Board Member*, Ibex Medical Analytics; Ozgur Mete: None

Background: Recent evidence suggests that alpha-inhibin positivity may be used to suggest VHL-driven pathogenesis in epithelial neuroendocrine neoplasms. The data on alpha-inhibin expression in paragangliomas and pheochromocytomas (PPGLs) is largely unknown. This study addresses this knowledge gap to further refine molecular immunohistochemistry.

Design: Retrospective review of our files identified 62 PPGLs (26 pheochromocytomas (PCCs) and 36 paragangliomas (PGLs)) with complete alpha-inhibin and SDHB immunoprofiles. These were correlated with clinicopathologic variables including catecholamine levels, tumor size, Ki67 LI, and the status of *RET* and *VHL* germline disease.

Results: Catecholamine levels were available for 39 (62.9%) PPGLs (15 PGLs and 24 PCCs). Genetic testing confirmed *VHL* in 5 PCCs and *RET* mutation in 1 PCC. Loss of SDHB expression, a surrogate marker of *SDHx*-driven pathogenesis, was found in 21 (35%) PPGLs (20 of 34 PGLs, 58%, and 1 of 26 PCCs, 3.8%); SDHB was indeterminate due to lack of internal control reactivity in 2 PGLs. Alpha-inhibin positivity was identified in 34 PPGLs (54.8%) including 25 (69.4%) PGLs and 9 (34.6%) PCCs. They included 19 (90.4%) SDHB-immunodeficient PPGLs (1 PCC and 18 PGLs) and 4 (80%) *VHL*-related PCCs. The two PGLs with indeterminate SDHB were also alpha-inhibin positive whereas the *RET*-driven PCC was negative. Tumors were assigned to a pseudohypoxic signature in the setting of *VHL*- or *SDHx*-related disease as well as in the absence mature secretory catecholamine phenotype (defined as lack of adrenergic or mixed adrenergic & noradrenergic phenotypes). Comparison of variables showed that alpha-inhibin expression was a significant feature of PPGLs with a pseudohypoxia signature. There was no statistical difference between the Ki67 LI and tumor size with respect to alpha-inhibin status in PPGLs, as well as within tumor subgroup analyses.

Conclusions: This discovery cohort provides the first evidence that alpha-inhibin expression in PPGLs strongly correlates with *VHL*- and *SDHx*-driven pseudohypoxic pathway disease. Validation of this finding in an independent series and with germline testing of other rare pseudohypoxia-related genes involved in the HIF- and Krebs cycle-pathways is needed to gain further insights into the predictive value of this finding.

597 Risk Stratification of Pediatric Patients with Tall-Cell Variant Papillary Thyroid Carcinoma

Anello Poma[1], Agnese Proietti[2], Clara Ugolini[2], Elisabetta Macerola[1], David Viola[2], Rossella Elisei[1], Fulvio Basolo[1]
[1]University of Pisa, Pisa, Italy, [2]University Hospital of Pisa, Pisa, Italy

Disclosures: Anello Poma: None; Agnese Proietti: None; Agnese Proietti: None; Agnese Proietti: None; Agnese Proietti: None; Agnese Proietti: None; Clara Ugolini: None; Elisabetta Macerola: None; David Viola: None; Fulvio Basolo: None

Background: The risk stratification of pediatric thyroid cancer is affected by the remarkable influence of age on the outcome of these tumors. As a consequence, the American Joint Committee on Cancer (AJCC) Tumor-Node-Metastasis (TNM) staging flatten pediatric tumors into low stages. However, pediatric thyroid carcinomas have a recurrence rate up to 30%, thus identifying those with a higher risk is crucial to differently manage young patients. The aim of the study was to investigate the impact of different risk stratification methods on pediatric patients with tall cell variant of papillary thyroid carcinoma (TCPTC), which is one of the most aggressive histological subtypes.

Design: From 2000 to 2017, 2027 patients were diagnosed with TCPTC at the University Hospital of Pisa. Among these, 32 (1.6%) were pediatric (age ≤18 years). Clinical pathological data was collected for all patients. In addition, follow-up data was available for 16 patients (median 4 years, range 1-13). American Thyroid Association (ATA) pediatric risk, age-metastasis-extent of disease-size of tumor (AMES) and metastasis-age-completeness of resection-invasion-size (MACIS) score were tested to predict recurrence-free survival of patients by log-rank test.

Results: According to the aggressiveness of the histological subtype, there were high rates of extra-thyroid extension (43.8%), vascular invasion (31.3%) and node metastasis (31.3%). All clinical pathological data are reported in table 1. No distant metastases occurred at diagnosis, thus all cases were AJCC stage I. No significant imbalances were observed between the original cohort and the subgroup of patients with follow-up data in terms of clinical pathological features. Five out of 16 patients (31.3%) had lymph node recurrence, four of

them within 2 years. ATA pediatric risk was the only significant stratification method in predicting recurrence (p=0.043, figure 1). AMES and MACIS score (cut-off 4) were not significant probably due to the limited sample size (p=0.072 and p=0.083 respectively). Among the other clinical pathological variables, male gender was associated with a higher risk of recurrence (p=0.054, figure 2).

Age	median 17 years (range 12-18)
Gender	7 (21.9%) males 25 (78.1%) females
Size	mean 1.64 cm ± 0.78
Tall cell (TC) component	21 (65.6%) >50% TC 11 (34.4%) 30%<tc<50%< p=""></tc<50%<>
Local invasion	14 (43.8%) extra-thyroid extension, 6 focal 11 (34.4%) thyroid capsule 6 (18.7%) thyroid parenchyma 1 (3.1%) tumor capsule
Vascular invasion	10 (31.3%) yes, 3 more than 4 foci 22 (68.7%) no
Multifocal	12 (37.5%) yes 20 (62.5%) no
Bilateral	7 (21.9%) yes 25 (78.1%) no
Thyroiditis	9 (28.1%) yes 23 (71.9%) no
Lymph nodes metastases	3 (9.4%) N1b 7 (31.9%) N1a 22 (68.7%) Nx
BRAF mutation	13 (76.5%*) p.V600E 4 (23.5%*) wild type 15 unknown

*on the total of tested cases.

Figure 1 - 597

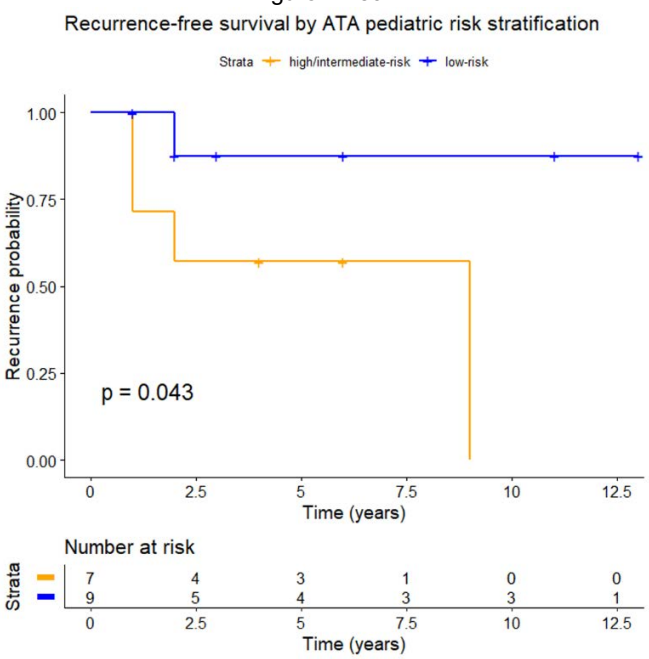

Figure 2 - 597

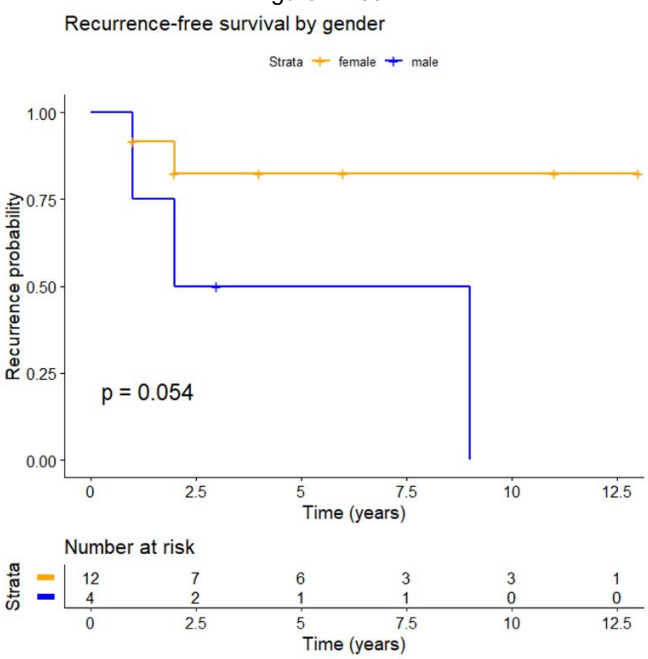

Conclusions: ATA pediatric risk is probably the best stratification method for thyroid pediatric TCPTC, but AMES and MACIS score could be useful. Finally, also gender should be considered to improve the current risk stratification.

598 Inconsistency of PAX8 Immunohistochemical Expression in Cribriform-Morular Variant of Papillary Thyroid Carcinoma

Mobeen Rahman[1], Christopher Griffith[2], Deborah Chute[3], Kathy Allen-Proctor[1]
[1]Cleveland Clinic Pathology and Laboratory Medicine, Cleveland, OH, [2]Cleveland Clinic Foundation, Cleveland, OH, [3]Cleveland Clinic, Cleveland, OH

Disclosures: Mobeen Rahman: None; Christopher Griffith: None; Deborah Chute: None; Kathy Allen-Proctor: None

Background: Cribriform-morular variant of papillary thyroid carcinoma (CMV-PTC) is a rare variant of papillary thyroid carcinoma that occurs sporadically or as a manifestation of familial adenomatous polyposis (FAP) syndrome. PAX8 is expressed in the thyroid anlage during development and is widely utilized as a reliable means of determining thyroid origin in instances of an unknown primary. Consistent expression of PAX8 is uniformly identified in other variants of papillary thyroid carcinomas but its use has only rarely been reported in CMV-PTC. We aspired to examine the immunohistochemical expression of PAX8 in CMV-PTC.

Design: Five different cases of CMV-PTC were obtained from the surgical pathology files of a large medical center with IRB approval. PAX8 immunochemistry was performed on representative sections of tumor (polyclonal rabbit antibody-10336-1-AP, ProteinTech Group, Inc.). Intact expression of PAX8 was defined as all tumor nuclei staining. Heterogenous expression of PAX8 was defined as partial PAX8 staining of all tumor nuclei. Absent expression of PAX8 was defined as complete absence of nuclear staining in the tumor.

Results: Of the five cases, two demonstrated intact nuclear expression of PAX8 (40%). Three cases demonstrated a heterogenous/partial nuclear expression of PAX8 (60%). The three cases with heterogenous/partial nuclear expression demonstrated positive staining in <5, 20, and 90% of the tumor cells. In all cases reviewed, the intensity of PAX8 staining in the uninvolved thyroid parenchyma was strong and diffuse.

Figure 1 - 598

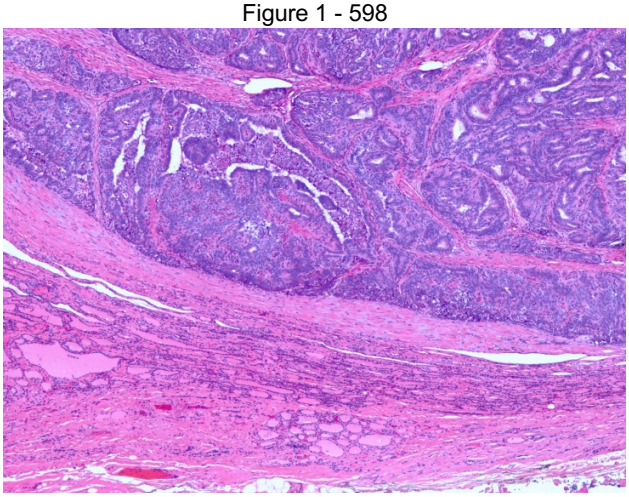

Figure 2 - 598

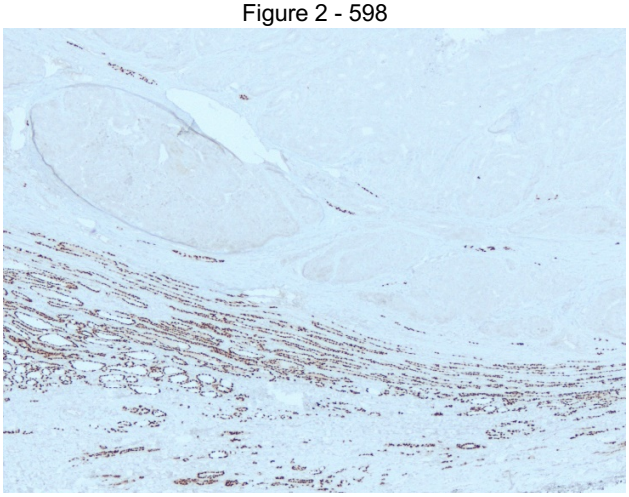

Conclusions: In addition to playing an important role in the development of the thyroid, PAX8 has consistent immunohistochemical expression in commonly encountered variants of papillary thyroid carcinomas (conventional, follicular, tall cell). In our series, there is partial/heterogenous expression of PAX8 in 60% of cribriform-morular variants of papillary thyroid carcinoma. Additionally, TTF1 and thyroglobulin are known to have inconsistent expression in CMV-PTC and therefore the possible lack of thyroid marker expression in these tumors is a potential diagnostic pitfall.

599 A Computational Strategy to Develop a Tall Cell Pipeline for Papillary Thyroid Carcinoma

Shabnam Samankan[1], Leah Militello[2], Sedef Everest[3], Binny Khandakar[4], Jihong Sun[5], Mark Urken[3], Scott Doyle[2], Margaret Brandwein-Weber[6]

[1]Mount Sinai Hospital Icahn School of Medicine, Alexandria, VA, [2]University at Buffalo, Buffalo, NY, [3]Mount Sinai Health System, New York, NY, [4]Mt Sinai St Luke's Roosevelt Hospital, New York, NY, [5]Mount Sinai West, New York, NY, [6]Icahn School of Medicine at Mount Sinai, New York, NY

Disclosures: Shabnam Samankan: None; Leah Militello: None; Sedef Everest: None; Binny Khandakar: None; Jihong Sun: None; Mark Urken: None; Scott Doyle: None; Margaret Brandwein-Weber: None

Background: Tall cell variant papillary thyroid carcinoma (TCV-PTC) is an aggressive histologic feature considered within the 2015 American Thyroid Association Risk of Recurrence guidelines, which impacts risk stratification and treatment decisions. TCV-PTC is currently defined as ≥ 30% tumor cells 2-3 times taller than wide by the World Health Organization (WHO). This diagnosis is made by microscopic visual estimation (VE), which suffers from interrater variability and begs for a computational approach. We compare VE with a computer-vision (CV) pipeline and hand annotations (HA) of minor and major cell axes to quantitatively measure “tallness”.

Design: Membranous βcatenin (βcat) expression was used to extract cell geometry. 30 PTC with variable tall cell populations were selected and IHC for βcat (Leica) was performed. Slides were digitized at 40x with an Olympus VS1206 scanner. Five observers classified cases by WHO standards into 3 groups (<10%, 10-29%, ≥ 30%) for H+E and βcat regions of interest (ROIs). Cohen’s kappa value (κ) for interrater agreement was calculated as $\kappa = (\rho_o - \rho_\epsilon)/(1- \rho_\epsilon)$, where ρ_o is the relative observed agreement, ρ_ϵ is probability of chance agreement. A subset of 5 tumors were hand annotated for minor / major cell axes. MATLAB R2019a was used to create the CV pipeline which also measured cell axes. Minor / major axis length ratios close to 0 indicate taller cells, while ratios close to 1 indicate rounder cells. Cells below a threshold of 0.5 were defined as “tall”.

Results: There was substantial interrater agreement for H+E and βcat ROI by VE (κ 73%, 69%, respectively). CV yielded lower average estimates of tall cells (16%) and HA yielded higher estimates (53%) compared with VE (**Figs 1, 2**). Using a threshold of 0.65 in the CV measurements shifted average tall cell component to 48%, bringing it closer to the HA measurements (**Table 1**). Comparing input with output tiles in the CV pipeline reveals that the different measurements are due to different cell detection and boundary segmentation criteria.

Table 1: **Tall cell percentage by measurement approach**

		Cut off for "Tall cell" by CV	
	HA	< 0.5	< 0.65
Average	53.0%	16.3%	48.4%
Minimum	46.5%	14.1%	46.3%
Maximum	58.8%	20.2%	50.2%

Figure 1 - 599

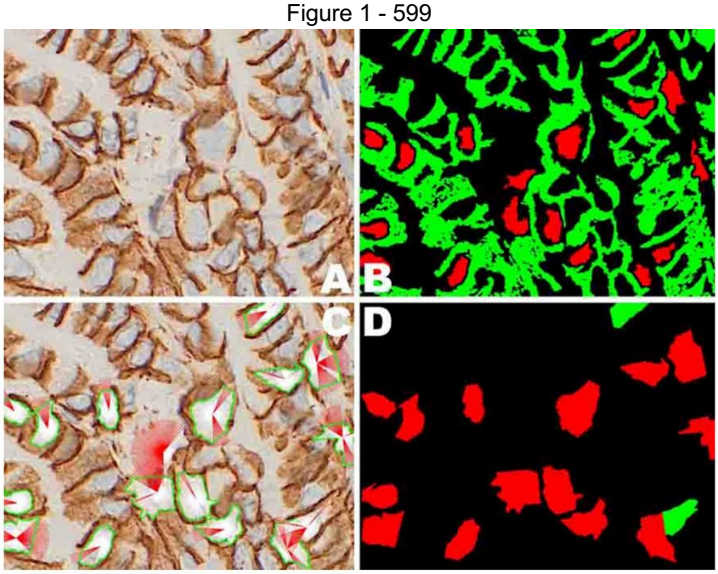

Fig1: A. Membranous βcat **B.** Nuclei (red), membranes (green). **C.** The ray function creates100 rays (max 50 pixels or 8.75 μ). White rays stop at the cell membrane pixels. Red rays are unbounded by membrane and truncated 50 pixels. If > 50% of rays are untruncated, the cell is eliminated. If the cell is not eliminated, endpoints connected as polygon (green). **D**. Green polygons represent tall cells, red represent non-tall cells.

Figure 2 - 599

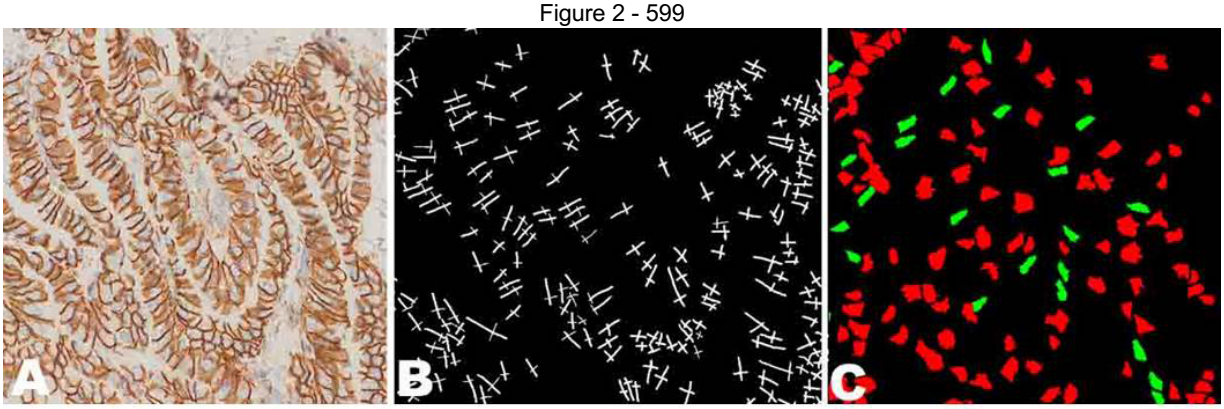

Fig 2: A. Membranous βcat **B.** HA **C.** Green polygons are tall cells, red are not tall.

Conclusions: Consistent, meaningful recognition of TCV-PTC requires a reproducible means of quantification. Our goal is to create a robust pipeline to be tested on entire digitalized PTC cases, linked to patient outcome. Future work will focus on adjudicating the different cell measurements in CV and HA, and comparing them with patient outcomes to develop a more quantitative and predictive TCV criteria.

600 Diagnostic Utility of INSM1 Immunohistochemistry in Medullary Thyroid Carcinoma

Jae Yeon Seok[1], Xuemo Fan[2]
[1]Gil Medical Center, Gachon University College of Medicine, Incheon, Korea, Republic of South Korea, [2]Cedars-Sinai Medical Center, Los Angeles, CA

Disclosures: Jae Yeon Seok: None; Xuemo Fan: None

Background: Insulinoma-associated protein 1 (INSM1), a transcription factor, is considered to be an emerging immunohistochemical marker for neuroendocrine tumors. Studies have demonstrated its high sensitivity and specificity in detecting neuroendocrine tumors in the head and neck and in various organs, but the diagnostic utility of INSM1 in medullary thyroid carcinoma (MTC) has not yet been fully investigated.

Design: Twenty one cases of MTC, 7 cases of MTC mimickers and 3 cases of c-cell hyperplasia from 2005 to 2019 were retrieved and immunostained for INSM1. The diverse histologic patterns of MTC was reviewed and correlated with the INSM1-immunoreactive pattern.

Results: All 21 MTC cases had a positive INSM1 nuclear immunoexpression with 70~95% tumor cells to be positive at moderate to strong intensity (B). The MTC mimickers include 3 papillary carcinomas with spindle cell or pleomorphic area, 2 poorly differentiated carcinomas, 1 follicular adenoma with atypical feature, and 1 nodular plasma cell hyperplasia. All 7 MTC mimickers were entirely negative for INSM1. Among diverse MTC histologic patterns, spindle cell area showed significant reduction in INSM1 expression (D) while papillary growth area was strong positive for INSM1 (F). Two out of 3 c-cell hyperplasia cases were positive for INSM1.

Figure 1 - 600

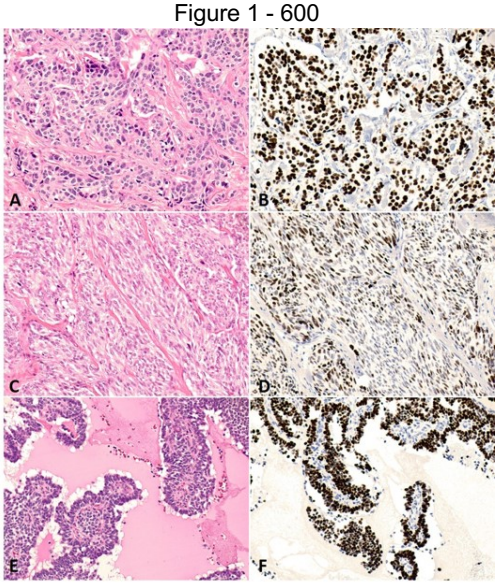

Conclusions: INSM1 is a novel and useful immunohistochemical marker for diagnosis of MTC with high sensitivity and specificity. A careful evaluation is needed in examining INSM1 expression in MTC with predominantly spindle cell pattern in which a significantly reduced immunoreactivity for INSM1 is observed.

601 How Reliable is the Ki-67 Proliferative Index in the Grading of Metastatic Well-Differentiated Neuroendocrine Neoplasms?

Hemlata Shirsat[1], Atreyee Basu[2], Navneet Narula[1], Andre Moreira[3], Fang Zhou[4]
[1]NYU Langone Health, New York, NY, [2]NYU Langone Medical Center, New York, NY, [3]New York Langone Health, New York, NY, [4]NYU School of Medicine, New York, NY

Disclosures: Hemlata Shirsat: None; Atreyee Basu: None; Andre Moreira: None; Fang Zhou: None

Background: When the first diagnosis of a well-differentiated neuroendocrine neoplasm (WDNEN) is made on a biopsy, crush artifact may impede mitotic counting, and the Ki-67 proliferative index (KPI) plays a more important role in grading. Few studies have examined the reliability of KPI in the grading of metastatic (met) WDNEN.

Design: Cases were retrieved from 2008-19. For each primary (1°) and met, a 40x hotspot image of a Ki-67 stained slide was taken. KPI was analyzed by the ImmunoRatio Plugin using ImageJ software. All were validated by independent manual counting. In 1 case, crush artifact precluded use of ImageJ. If multiple mets were present, the largest was selected. Cytology and cases with fewer than 100 cells were omitted. Tumors were graded as G1(KPI<3%), G2(KPI 3-20%), or G3(KPI>20%). Grade and KPI were compared between each 1° and met.

Results: 67 cases, including 38 mets from 29 1° WDNEN, were evaluated. There were 12, 2, 2, 1, 17, and 4 mets from lung, thymus, middle ear, pancreas, small bowel, & colon respectively. The greatest variations in KPI from 1° to met were seen in lung compared to all other sites.

In 24/38(63%) of all mets, the grade was the same as 1°. In 14/38(37%) of all mets, the grade was different: 4/14(29%) were lower while 10/14(71%) were higher than 1°. In mets from lung, 2 had lower, 6 had the same, & 4 had higher grade. In mets from middle ear, the grades increased. In mets from small bowel 2 had lower, 12 had the same, and 3 had higher grade. In mets from colon 3 had the same and 1 had higher grade. And in mets from thymus & pancreas, the grades remained the same. See Fig 1.

3 mets were diagnosed before 1° (2 days to 2 months). Mets with higher grade than 1° tended to have longer time interval between 1° and met, but this was not significant at the 95% confidence level (Kruskal-Wallis test, p=0.08).

28 mets were regional and 10 were distant. There was no correlation between met site and grade change (Person Chi-square, p=0.33). Also see Table 1.

Patient #	Primary Dx	Sex	Age	Primary			Metastasis			ΔKPI & grade change from primary to met	Years from primary to met
				Primary site	KPI(%) and grade	Specimen type	Met site	KPI(%) and grade	Specimen Type		
1	TC	F	67	lung	5.4 G2	exc	regional LN	1.2 G1	exc	-4.2 G2-->G1	0.0
2	AC	F	71	lung	39.7 G3	exc	regional LN	11.9 G2	exc	-27.8 G3-->G2	0.0
3	AC	F	63	lung	14 G2	exc	regional LN	4 G2	exc	-10 same (G2)	0.0
4	AC	F	68	lung	6.7 G2	exc	liver	17.9 G2	bx	+11.2 same (G2)	4.4
4	AC	F	68	lung	6.7 G2	exc	regional LN	5.2 G2	exc	-1.5 same (G2)	0.0
5	TC	M	52	lung	1.3 G1	exc	regional LN	1.5 G1	exc	+0.2 same (G1)	0.0
6	AC	F	56	lung	2.1 G1	exc	regional LN	1.1 G1	exc	-1.3 same (G1)	0.0
7	TC	f	65	lung	0 G1	exc	pleura	0 G1	exc	0 same (G1)	2 days before
8	AC	F	61	lung	2.9 G1	exc	regional LN	6 G2	exc	+3.1 G1-->G2	0.0
8	AC	F	61	lung	2.9 G1	exc	liver	10.6 G2	bx	+7.7 G1-->G2	4.2
9	TC	F	60	lung	1.7 G1	exc	regional LN	3.6 G2	exc	+1.9 G1-->G2	0.0
10	AC	M	58	lung	19.5 G2	exc	regional LN	34.5 G3	exc	+15 G2-->G3	0.0
11	AC	M	63	thymus	10.3 G2	exc	pericardium	13.6 * G2	bx	+3.3 same (G2)	0.0
11	AC	M	63	thymus	10.3 G2	exc	regional LN	9 G2	bx	-1.3 same (G2)	2 months before
12	MEA	F	32	middle ear	1.4 G1	exc	brain	8.4 G2	exc	+7 G1-->G2	7.6
12	MEA	F	32	middle ear	1.4 G1	exc	regional LN	4.3 G2	exc	+2.9 G1-->G2	6.8
13	WD2	M	74	pancreas	8.7 G2	exc	regional LN	5.5 G2	exc	-3.2 same (G2)	0.0
14	WD2	F	52	small bowel	3.4 G2	exc	regional LN	2 G1	exc	-1.4 G2-->G1	0.0
15	WD2	F	50	small bowel	5.1 G2	exc	regional LN	2.3 G1	exc	-2.8 G2-->G1	0.0
16	WD2	M	51	small bowel	2.5 G1	exc	regional LN	2 G1	exc	-0.5 same (G1)	0.0
17	WD2	F	50	small bowel	1.6 G1	exc	regional LN	1.6 G1	exc	0 same (G1)	0.0
18	WD2	M	61	small bowel	2.5 G1	exc	regional LN	1.6 G1	exc	-0.9 same (G1)	0.0
19	WD1	M	62	small bowel	1.6 G1	exc	regional LN	0 G1	exc	-1.6 same (G1)	0.0
19	WD1	M	62	small bowel	1.6 G1	exc	liver	0 G1	exc	-1.6 same (G1)	1.4
20	WD1	M	63	small bowel	1.4 G1	exc	regional LN	2.6 G1	exc	+1.2 same (G1)	0.0
20	WD1	M	63	small bowel	1.4 G1	exc	liver	1.2 G1	bx	-0.2 same (G1)	3.8
21	WD1	M	62	small bowel	1.5 G1	exc	regional LN	1.3 G1	exc	-0.2 same (G1)	0.0
22	WD2	M	47	small bowel	2.1 G1	exc	liver	2.1 G1	bx	0 same (G1)	20 days before
23	WD1	M	72	small bowel	2.4 G1	exc	regional LN	1.6 G1	exc	-0.8 same (G1)	0.0
24	WD1	M	33	small bowel	1.9 G1	exc	regional LN	1.5 G1	exc	-0.4 same (G1)	0.0
25	WD2	F	54	small bowel	1.4 G1	exc	regional LN	1.1 G1	exc	-0.3 same (G1)	0.0
26	WD2	M	70	small bowel	2 G1	exc	regional LN	3.9 G2	bx	1.9 G1-->G2	4.8
26	WD2	M	70	small bowel	2 G1	exc	liver	10.3 G2	bx	8.3 G1-->G2	4.8
27	WD1	F	21	small bowel	1.3 G1	exc	regional LN	6.6 G2	exc	5.3 G1-->G2	0.0
28	WD1	F	47	colon	1.6 G1	exc	peritoneal implant	1.8 G1	exc	0.2 same (G1)	1.8
28	WD1	F	47	colon	1.6 G1	exc	ovary	1.6 G1	exc	0 same (G1)	1.8
28	WD1	F	47	colon	1.6 G1	exc	regional LN	1.6 G1	exc	0 same (G1)	1.8
29	WD1	M	82	colon	2.5 G1	exc	regional LN	3.8 G2	exc	1.3 G1-->G2	0.0

Abbreviations: AC: atypical carcinoid. Bx: biopsy. Exc: excision. LN: lymph node. MEA: middle ear adenoma. Met: metastasis. TC: typical carcinoid. WD1: grade 1 well-differentiated neuroendocrine tumor. WD2: grade 2 well-differentiated neuroendocrine tumor.
*Pericardial met from patient 11 was crushed and had manual KPI analysis only. All other data in this chart is from ImageJ analysis.

Figure 1 - 601

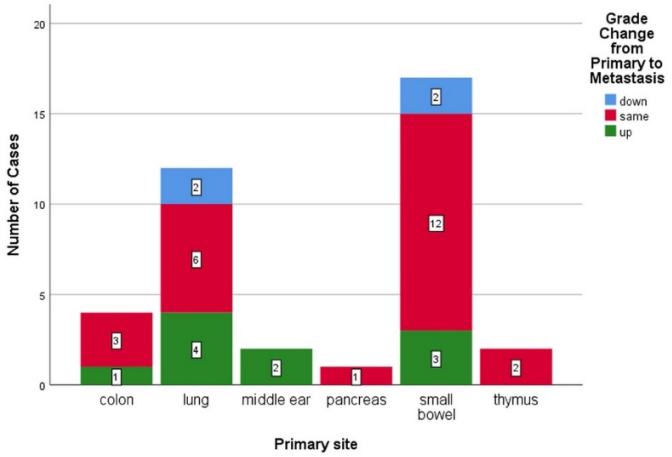

Figure 2 - 601

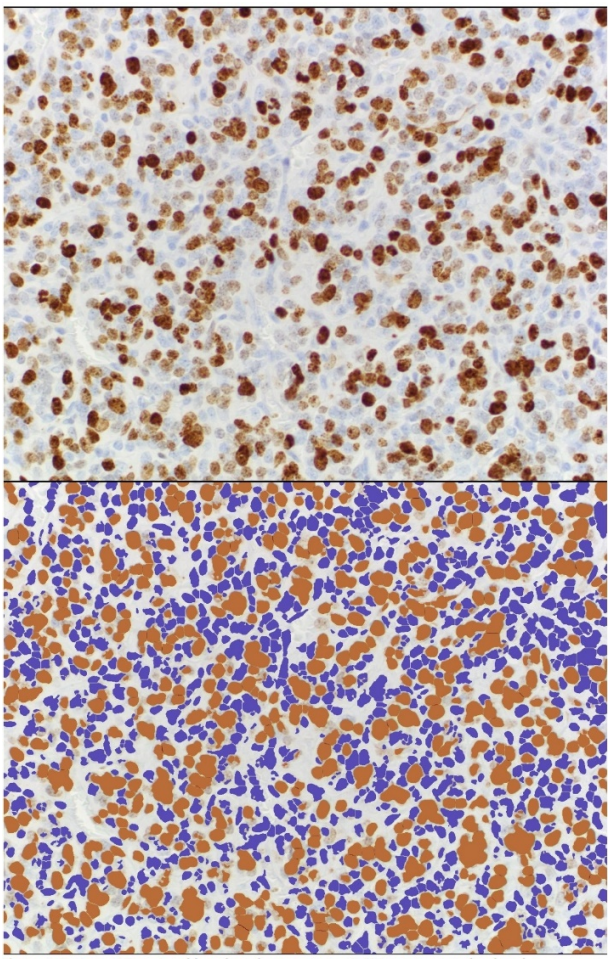

Figure 2: Patient #10, regional lymph node metastasis. Ki-67 immunostain (top) and ImmunoRatio output in ImageJ (bottom). The KPI in the lymph node metastasis was 34.5% compared to 19.5% in the lung primary. If the lymph node metastasis had been received as a crushed biopsy, small cell carcinoma may have entered the differential.

Conclusions: Our study showed that in most met WDNEN (63%), the grade remained the same as the 1°. The grade was higher in 10/38(26%) and lower in 4/38(11%). There was a trend toward higher grade in mets that occurred at a longer time interval after the 1°. Fig 2 shows a potential diagnostic pitfall when the met shows much higher KPI than 1°. In conclusion, if a met WDNEN is suspected as a first-time diagnosis, KPI must be used cautiously for classification of WDNEN since over/under-grading may occur.

602 Long Noncoding RNA Expression in Adrenal Cortical Neoplasms

Oyewale Shiyanbola[1], Toshi Kinoshita[2], Heather Hardin[3], Ricardo Lloyd[4]
[1]University of Wisconsin Hospital and Clinics, Madison, WI, [2]School of Medicine and Public Health, The University of Wisconsin-Madison, Madison, WI, [3]University of Wisconsin-Madison, Madison, WI, [4]University of Wisconsin, Madison, WI

Disclosures: Oyewale Shiyanbola: None; Heather Hardin: None; Ricardo Lloyd: None

Background: Long noncoding RNAs (lncRNAs) participate in transcription and in epigenetic or posttranscriptional regulation of gene expression; they also have a role in carcinogenesis. Adrenal cortical neoplasms often represent challenging diagnostic problems in pathology, because it is often difficult to distinguish between adrenal cortical adenomas and carcinomas. Adrenal cortical carcinomas are aggressive malignancies with high rates of recurrences following surgical treatment. LncRNAs may have a role in the development and progression of adrenal cortical neoplasms. We examined a group of adrenal cortical neoplasms to determine the role of specific lncRNAs in tumor development, progression and classification.

Design: Two lncRNAS, including metastasis-associated lung adenocarcinoma transcript 1(*MALAT1*) and psoriasis-susceptibility related RNA gene induced by stress (*PRINS*) were used for *in situ* hybridization (ISH) analysis on a tissue microarray (TMA) and quantitative real-time polymerase chain reaction (qRT-PCR). The TMA consisted of 1 mm duplicate cores of normal adrenal cortex (NAC) (n=22), adrenal cortical adenomas (ACAs) (n= 100)), and adrenal cortical carcinomas (ACCs) (n=20). ISH was performed with RNAScope technology (Advanced Cell Diagnostics). The results of ISH were analyzed manually and by Vectra imaging technology with quantification using Nuance and inForm software. qRT-PCR was done using some of the same tissue blocks used for construction of the TMA.

Results: ISH showed predominantly nuclear expression of both lncRNAs in normal and neoplastic adrenal cortical tissues. MALAT1 was most highly expressed in ACCs compared to NAC and ACA ($p<0.001$). PRINS was more highly expressed in NACs and ACAs compared to ACCs ($p<0.05$). qRT-PCR analysis supported the ISH findings.

Conclusions: The lncRNAs *MALAT1 and PRINS* have regulatory roles in adrenal cortical tumor development. *MALAT1* appears to have an oncogenic role in adrenal cortical tumor progression while PRINS may have a tumor suppressor-like role in adrenal cortical neoplastic development. These lncRNAs may serve as potential diagnostic and therapeutic targets for ACCs.

603 An Investigation into Low Suspicion Thyroid Imaging Reporting and Data System (TI-RADS) Nodules with Fine Needle Aspiration (FNA) Cytology, Molecular and Surgical Pathology Findings

Wei Sun[1], Joseph Yee[2], Yan Shi[1], Oliver Szeto[3], Aylin Simsir[4], Tamar Brandler[5]
[1]New York University Langone Medical Center, New York, NY, [2]NYU Langone Medical Center, Woodside, NY, [3]NYU Langone Health, New York, NY, [4]New York University School of Medicine, Edison, NJ, [5]NYU Langone Health, Highland Park, NJ

Disclosures: Wei Sun: None; Joseph Yee: None; Yan Shi: None; Oliver Szeto: None; Aylin Simsir: None; Tamar Brandler: None

Background: The American College of Radiology (ACR) 2017 Thyroid Imaging Reporting and Data System (TI-RADS) added a new risk stratification system for classifying thyroid nodules based on sonographic appearance (T1-T5). FNA is generally not recommended for benign or low suspicion nodules. However, other factors such as nodule size and family history may trigger an order for an FNA. Our study aimed to examine the cytologic diagnosis, molecular profiles and surgical follow up in a select group of patients with sonographically benign appearing thyroid nodules.

Design: We performed a retrospective review in our pathology database of cases from 1/1/2016-4/1/2018, prior to our institution's adoption of the TI-RADS classification system. Thyroid nodules with in-house ultrasound exam (US), FNA cytology, The Bethesda System (TBS) cytology diagnosis, molecular testing, and surgery were included. The USs from these cases were retrospectively reviewed and assigned TI-RADS scores (TR1-TR5) by a board certified radiologist. There were no TR1 nodules. TR2 (not suspicious) and TR3 (mildly suspicious) nodules were selected for evaluation.

Results: From 1/1/2016-4/1/2018, there were a total of 34 patients that fit the selection criteria. Of these, there were 5 TR2 thyroid nodules and 29 TR3 thyroid nodules with corresponding FNA TBS, molecular and surgical diagnoses (table1).

Table 1: Cytology, Surgical and Molecular Diagnoses with Demographic Data on TI-RADS- TR2 and TR3 nodules			
		TR2 (n = 5)	**TR3** (n = 29)
Age Range (mean)		25 - 84 (44.8)	26 - 77 (48.7)
Gender Male : Female		1:4	4:25
Thyroid Nodule Size Range (mean)		0.9 cm - 3.4 cm (2.7 cm)	1.0 cm - 4.5 cm (2.3 cm)
Cytology Diagnosis	TBS III	n = 3	n = 23
	TBS IV	n = 1	n = 5
	TBS V	n = 1	n = 1
Surgical Diagnosis	Thyroid Cancer	n = 2 (40%)	n = 6 (20.7%)
	NIFTP	n = 1 (20%)	n = 13 (44.8%)
	Benign (Follicular Adenoma or Benign Thyroid nodule)	n = 2 (40%)	n = 10 (34.5%)
Molecular Findings		Negative = 1 BRAF = 1 D1CER1 = 1 PAX8/PPARG = 1 Gene Expression Profile = 1	Negative = 4 RAS = 17 EIF1AX = 2 MET = 2 PAX8/PPARG = 2 TP53 = 2
Key: TBS III= Atypia of undetermined significance/follicular lesion of undetermined significance (AUS/FLUS); **TBS IV**= Follicular neoplasm or suspicious for a follicular neoplasm; **TBS V**= Suspicious for Malignancy; **NIFTP**= Noninvasive follicular thyroid neoplasm with papillary-like features			

Conclusions: Our study shows that sonographically benign appearing/low suspicion thyroid nodules may display molecular alterations; 50% of those proved to be RAS mutations in our study. Approximately 60% of aspirated TR2 nodules and 66% of TR3 nodules were malignant or NIFTP on excision. Despite their lower suspicion index on US, with lower TI-RADS scores, benign appearing nodules on US need to be evaluated in the context of clinical, cytologic and molecular information in order to determine clinical course.

604 Identification of Recurrent TERT Promoter Mutations in Intrathyroid Thymic Carcinomas

Ippei Tahara[1], Naoki Oishi[2], Kunio Mochizuki[2], Toshio Oyama[3], Kazuyuki Miyata[4], Akira Miyauchi[5], Mitsuyoshi Hirokawa[5], Ryohei Katoh[6], Tetsuo Kondo[2]

[1]Chuo City, Yamanashi Prefecture, Japan, [2]University of Yamanashi, Chuo, Yamanashi, Japan, [3]Yamanashi Prefectural Central Hospital, Kofu, Yamanashi, Japan, [4]Kofu Municipal Hospital, Kofu, Yamanashi, Japan, [5]Kuma Hospital, Kobe, Hyogo, Japan, [6]Ito Hospital, Shibuya-ku, Japan

Disclosures: Ippei Tahara: None; Naoki Oishi: None; Kunio Mochizuki: None; Mitsuyoshi Hirokawa: None; Tetsuo Kondo: None

Background: Intrathyroid thymic carcinoma (ITTC), also called carcinoma showing thymus-like elements (CASTLE) is a very rare malignant neoplasm, accounting for 0.1-0.15% of all malignant thyroid neoplasms. ITTC histologically and immunophenotypically resembles thymic carcinoma (TC). For instance, the tumor cells generally show immunopositivity for KIT and CD5. Given the limited understandings on the genetics of ITTC, genetic characterization of ITTC may provide novel insights into the unique clinicopathological features of this rare disease. In this study, we investigated the clinicopathological, histopathological, immunohistochemical, and genetic features of ITTCs comparing with TC.

Design: We collected 9 ITTCs and 8 TCs. We reviewed the histopathology and obtained following clinicopathological data from the medical records: age, sex, tumor size (cm), TNM classification, lymph node (LN) metastasis, and distant metastasis. Immunohistochemistry (IHC) for KIT, CD5, p63, TTF-1, thyroglobulin, PAX8, EGFR, Ki67, PD-L1, p53 and *in situ* hybridization for EBER (ISH-EBER) were carried out. We further investigated mutation status of key oncogenic genes including *KIT*, *EGFR*, *BRAF* and *TERT* promoter using standard Sanger sequencing.

Results: ITTCs affected significantly younger patients than TCs: 54.2±9.3 vs 66.8±9.6, p = 0.043, Mann-Whitney test. There were no other significant differences in clinical characteristics of ITTCs and TCs. IHC showed similar immunophenotype of ITTCs and TCs: KIT, 100% (9/9) in ITTCs vs. 100% (8/8) TCs; CD5, 100% (9/9) vs. 100% (8/8); p63 100% (9/9) vs. 88% (7/8). TTF-1, thyroglobulin, PAX8 and ISH-EBER were all negative in both categories. EGFR showed statistical significance, Ki67 and PD-L1 showed no statistical significance (Table 1). Thus ITTCs included more p53 overexpression (cut off 60% positivity) cases than TCs: 78% (7/9) vs 25% (2/8). Genetic analysis identified *TERT* promoter C228T mutation specifically in 22% (2/9) of ITTCs but not in TCs. *EGFR* mutations were seen in 11% (1/9) of ITTCs and 25% (2/8) of TCs. *KIT* mutations and *BRAFV600E* were not identified in both ITTCs and TCs. Comparing 2 *TERT* promoter mutated ITTCs with other I

	No. of cases	positive cases							Overexpression	% of positive cells (mean±SD)	% of positive cells (mean±SD)	H-score (mean±SD)
		KIT	p63	CD5	EBER	TTF-1	TG	PAX8	P53	Ki67	EGFR	PD-L1
ITTC	9	9(100%)	9(100%)	9(100%)	0	0	0	0	7(78%)	47.2±23.3	28.1±25.3	33.3±33.6
TC	8	8(100%)	7(88%)	8(100%)	0	0	0	0	2(25%)	34.4±25.9	63.1±26.3	62.4±42.3
										$p = 0.26$	$p = 0.03$	$p = 0.10$

Conclusions: We indicated ITTCs and TCs have similar histological and genetic character, except for EGFR, p53 over expression and *TERT* promoter mutation. Our study showed no mutation of *TERT* promoter in TCs. Based on the results, *TERT* promoter mutation may delineate a distinct molecular pathogenesis of ITTCs.

605 Clinicopathologic Features of Warthin-like Variant of Papillary Thyroid Carcinoma (WL-PTC): A Retrospective Analysis of a Rare Entity from a Large Academic Institution

Tuyet Hong Tran[1], Cheng Liu[2], Fang Zhou[3], Tamar Brandler[4]
[1]New York University Langone Medical Center, New York, NY, [2]NYU Langone Medical Center, New York, NY, [3]NYU School of Medicine, New York, NY, [4]NYU Langone Health, Highland Park, NJ

Disclosures: Tuyet Hong Tran: None; Fang Zhou: None; Tamar Brandler: None

Background: Little is known about Warthin-like variant of papillary thyroid carcinoma (WL-PTC). Its clinicopathologic features are thought to be similar to the classic variant of papillary thyroid carcinoma (PTC). Our aim was to evaluate clinical histories, laboratory findings, cytologic (FNA) and histopathologic features to better understand and characterize WL-PTC.

Design: We performed a retrospective review of PTC resection cases from 2013-2019 in our pathology database. Cases with a predominant WL-PTC pattern were chosen for further review. Corresponding clinical histories, laboratory results, and FNA cases were assessed.

Results: Of 3,731 thyroid surgical resection cases, 1,671 were diagnosed with PTC. 25/1,671 were reported to have Warthin-like features, but only 15/25 cases displayed Warthin-like features in >50% of tumor cells and were included in our study (Table 1). 80% were white, 6.7% Asian/Pacific Islander and 13.3% did not report race. 3/15 FNA cases were Bethesda III due to few follicular cells with nuclear atypia in a background of lymphocytes, making it difficult to distinguish atypia from PTC (Figs 1a-d). On resection, all cases had concomitant Hashimoto thyroiditis (HT). All cases tested for BRAF V600E immunohistochemistry were positive (4/4). All 5/15 cases with lymph node metastases had coexisting classic or tall cell features, though not all cases with classic or tall cell features metastasized. 46.7% required post-operative radioactive iodine therapy. To date, the median survival is 100% (range 1 to 6 years).

Table 1. Clinicopathologic features of Warthin-Like PTC (cases from 2013 to 2019)

Case	Sex (M/F) / Age (years)	Presentation	Laboratory Findings	Cytology Diagnosis	Cytology Background	Tumor Size (cm)	BRAF V600E IHC	Other minor features	Lymph Node Metastasis	TMN Staging
1	F / 60	Concern of neck mass	anti-TPO 2583.5, anti-Tg 233.6	Bethesda VI	Lymphocytes, histiocytes	3.0	Positive	Classic	Level I, II, III and VI	T3N1b
2	F / 69	Incidental US finding	anti-TPO 54, anti-Tg 36	Bethesda VI	Multinucleated giant cells	1.8	N/A	Tall cell	Level III	T3N1b
3	F / 69	Concern of neck mass	anti-TPO 62, anti-Tg <0.1	Bethesda VI	N/A	4.2	N/A	Tall cell	Level III	T4aN1b
4	F / 62	Palpable nodule on exam	N/A	Bethesda VI	Lymphocytes, histiocytes, multinucleated giant cells	4.5	N/A	Classic	N/A	T3N0
5	F / 52	Palpable nodule on exam	anti-TPO 12, anti-Tg 516	Bethesda VI	Multinucleated giant cells	2.2	N/A	N/A	N/A	T2N0
6	F / 40	Palpable nodule on exam	N/A	Bethesda VI	N/A	1.8	N/A	Tall cell	Level VI	T3N1a
7	F / 45	Thyromegaly on exam	N/A	Bethesda VI	N/A	0.9	N/A	N/A	N/A	T1aN0
8	F / 32	Palpable nodule on exam	anti-TPO high*	Bethesda VI	Multinucleated giant cells	1.3	N/A	Tall cell	N/A	T1bN0
9	F / 24	Palpable nodule on exam	anti-TPO 821.40, anti-Tg 403.1	Bethesda VI	Multinucleated giant cells, macrophages	1.6	Positive	Classic	N/A	T1bN0
10	F / 58	Thyromegaly on exam	anti-TPO 845.9, anti-Tg 21.6	Bethesda VI	Lymphocytes, multinucleated giant cells	1.2	N/A	N/A	N/A	T1bN0
11	F / 45	Palpable nodule on exam	anti-TPO 5901.5, anti-Tg 275.2	Bethesda VI	N/A	0.7	N/A	N/A	N/A	T2N0
12	F / 42	Incidental US finding	anti-TPO elevated*	Bethesda III	Lymphocytes	0.5	N/A	N/A	N/A	T1aN0
13	F / 60	Incidental US finding	N/A	Bethesda III	Lymphocytes, multinucleated giant cells	0.8	N/A	Classic	N/A	T1aN0
14	F / 56	Incidental US finding	anti-TPO 630, anti-Tg >1000	Bethesda VI	Multinucleated giant cells	1.8	Positive	Classic	Level II, III and IV	T2N1b
15	F / 57	Concern of neck mass	N/A	Bethesda III	Lymphocytes, histiocytes, multinucleated giant cells	1.8	Positive	Classic	N/A	T1bN0

Key:

anti-thyroid peroxidase antibodies (anti-TPO) [normal 0-5.0 IU/mL]

anti-thyroglobulin antibodies (anti-Tg) [normal 0-4.0 IU/mL]

Atypia of Undetermined Significance/ Follicular Lesion of Undetermined Significance, AUS/FLUS (Bethesda III)

Positive for malignancy (Bethesda VI)

Figure 1 - 605

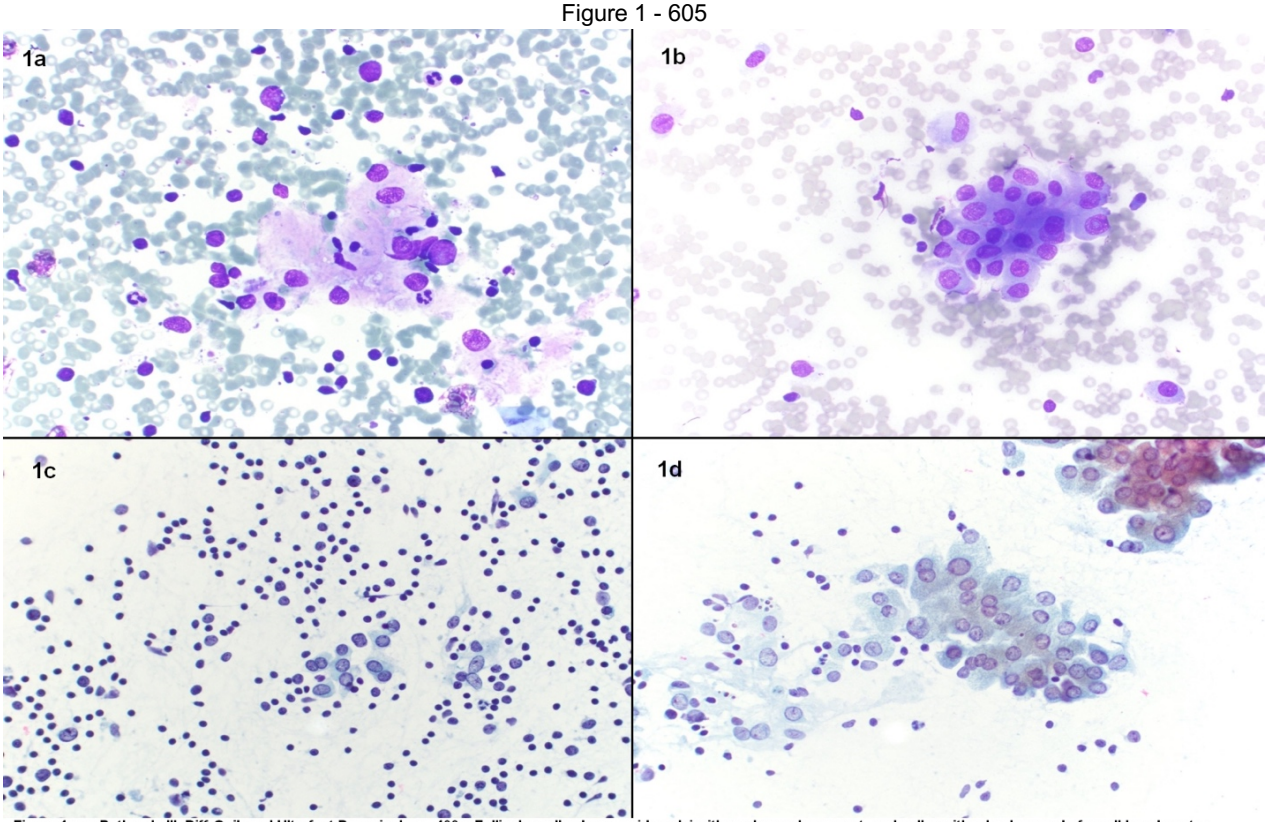

Figure 1a, c. Bethesda III, Diff-Quik and Ultrafast Papanicolaou, 400x. Follicular cells show ovoid nuclei with nuclear enlargement, and pallor with a background of small lymphocytes. Figure 1b, d. Bethesda VI, Diff-Quik and Ultrafast Papanicolaou, 400x. PTC tumor cells showing abundant dense granular cytoplasm with ovoid nuclei, nuclear enlargement, overlapping, pallor, grooves, and irregularity with occasional nuclear pseudoinclusions with a background of small lymphocytes.

Figure 2 - 605

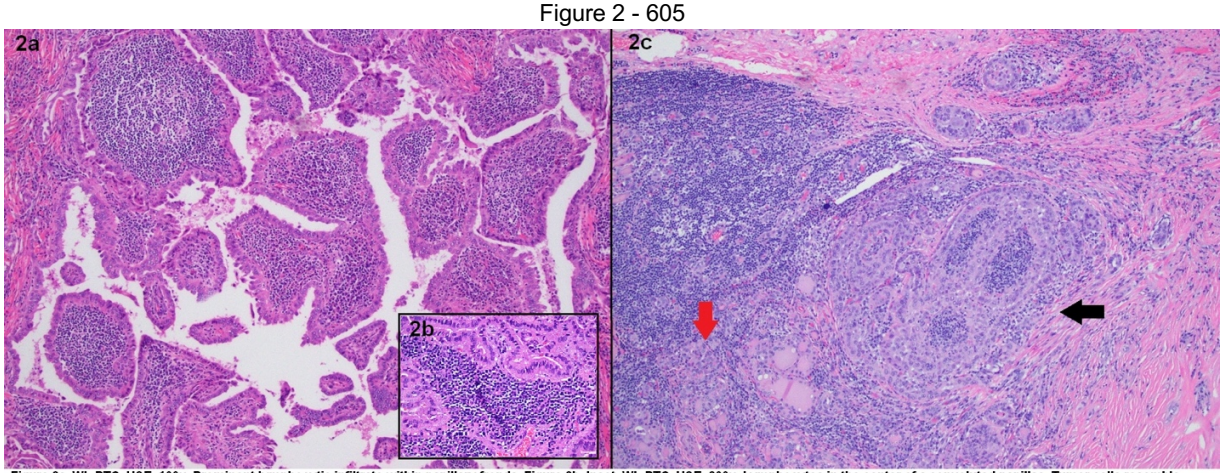

Figure 2a. WL-PTC, H&E, 100x. Prominent lymphocytic infiltrate within papillary fronds. Figure 2b. Inset, WL-PTC, H&E, 200x. Lymphocytes in the center of a convoluted papillae. Tumor cells resemble tall cell variant with "tall cell change" but lack features such as distinct cell borders. Figure 2c. WL-PTC, H&E, 100x. Endocrine atypia (red arrow) adjacent to WL-PTC microcarcinoma (black arrow).

Conclusions: Of all PTC resections at our institution 0.9% were WL-PTC. WL-PTC cases had a prominent lymphocytic infiltrate within papillary fronds and oncocytic cytoplasm (Fig 2a). The unique histologic features of WL-PTC add unique challenges to its diagnosis. Due to its strong association with HT, WL-PTC, particularly microcarcinomas, may be overlooked as endocrine atypia (Fig 2c). As WL-PTC possesses oncocytic features, it can resemble tall cell variant PTC which has a poorer prognosis (Fig 2b). Moreover, minor co-existing tall cell components can actually occur in some WL-PTCs. Foci with tall cell features should be distinguished from WL-PTC by lack of lymphocytic infiltrate within long papillae, and taller than wide cells with distinct cell borders. Like the classic variant, WL-PTC has a favorable prognosis. Metastasis seems to be associated with the presence of classic or tall cell features. More studies are needed to further elucidate this association.

606 Second Opinion in Thyroid Pathology, an Institutional Experience at a Large Head and Neck and Endocrine Cancer Referral Center

Anna Trzcinska[1], Nishant Agrawal[1], David Sarne[1], Peter Angelos[1], Nicole Cipriani[1]
[1]The University of Chicago, Chicago, IL

Disclosures: Anna Trzcinska: None; Nishant Agrawal: None; David Sarne: None; Peter Angelos: None; Nicole Cipriani: None

Background: The importance of second opinion in diagnosis of thyroid lesions has been evaluated, with published discrepancy rates of 10-22%. The aim of this study is to present an institutional experience with second opinion in thyroid diagnosis at a major head and neck and endocrine cancer referral center, in order to further elucidate discrepancy rates and identify areas of thyroid pathology most likely subject to diagnostic variability with resultant potential change in treatment or prognosis.

Design: The pathology database was searched for consultation or referral cases performed between 2013-2019. Lobectomies, hemithyroidectomies, completion thyroidectomies, and total thyroidectomies were included. Fine needle aspiration and core biopsies were excluded. Cases were excluded if a change in diagnosis at the time of second opinion was due to changes in classification that post-dated the original diagnosis. Outside reports were compared to final internal diagnoses. The results were grouped into major change, minor change, and no change categories. A major change was defined as a benign-malignant reclassification or a reclassification of a cancer type. A minor change was defined as a change in stage, margins, or vascular invasion. Missed papillary thyroid microcarcinoma or C-cell hyperplasia was considered minor.

Results: Search yielded 134 cases reviewed by a single pathologist. 100 came from community hospitals or private pathology groups, and 34 came from academic medical centers. A major change was made in 31 cases (23%), minor in 44 (33%), and no change in 59 (44%). A major change occurred in 23% of cases from community/private groups and 24% of cases from academic centers. Of major changes, the diagnosis was changed from malignant to non-malignant in 13, from benign to malignant in 2, and a cancer type reclassification was made in 16. The most common malignancy change was from follicular variant of papillary to adenoma or NIFTP (7 cases). The most common cancer type change was from well- to poorly-differentiated carcinoma (10 cases). Oncocytic histologic features were mentioned in 13 (42%) of the major change cases, suggesting an area of controversy.

Conclusions: Thyroid neoplasia remains challenging and subject to observer variability. Second opinion may result in diagnostic changes with significant treatment and prognostic implications for patients.

607 Papillary Thyroid Carcinoma with High Grade Features Versus Poorly Differentiated Thyroid Carcinoma: An Analysis of Clinicopathologic and Molecular Features and Outcome

Kristine Wong[1], Fei Dong[1], Justine Barletta[2], Michelle Afkhami[3], Milhan Telatar[3]
[1]Brigham and Women's Hospital, Boston, MA, [2]Brigham and Women's Hospital, Harvard Medical School, Boston, MA, [3]City of Hope National Medical Center, Duarte, CA

Disclosures: Kristine Wong: None; Fei Dong: None; Justine Barletta: None; Michelle Afkhami: None; Milhan Telatar: None

Background: Similar to poorly differentiated thyroid carcinoma (PDTC), papillary thyroid carcinoma (PTC) with high grade features (HGF) demonstrates increased mitotic activity and/or necrosis; however, PTC HGF are excluded from the WHO definition of PDTC based on maintained nuclear features of PTC. The goal of this study was to compare the clinicopathologic and molecular features and clinical outcome of PTC HGF and PDTC.

Design: Consecutive tumors diagnosed between 2005 and 2019 that met criteria for PTC HGF (defined as tumors with maintained nuclear features of PTC and mitoses numbering 5 or more per 10 HPF and/or tumor necrosis) and PDTC (defined per WHO criteria: solid/insular/trabecular growth, lack of nuclear features of PTC, and 3 or more mitoses per 10 HPF, tumor necrosis, or convoluted nuclei) were identified. Clinicopathologic characteristics and follow-up data were recorded. Targeted next generation sequencing was performed on cases with material available. The presence of driver mutations, likely pathogenic secondary alterations, fusions, and copy number alterations (CNA) were recorded.

Results: Our cohort includes 15 PTC HGF and 47 PDTC. Both patient groups had a similar age at diagnosis and female to male ratio. The mean tumor size was also similar; however, PTC HGF was associated with a higher rate of T4 disease (53% vs. 13%, p=0.0027) and lymph node metastases (73% vs. 38%, p=0.049). The disease-free survival (DFS) was significantly worse for patients with PTC HGF compared to those with PDTC using Kaplan-Meier estimation (p=0.0034). For patients with sufficient follow-up data who were M0 at diagnosis, the 1-, 2-, and 5-year DFS was 67%, 44%, and 0% for PTC HGF and 86%, 81%, and 67% for PDTC. PTC HGF had a significantly higher rate of activating *BRAF* mutations (50% vs. 6%; p=0.0024) and a trend toward more gene fusions (25% vs. 3%; p=0.052); whereas the *RAS* mutation rate was similar between groups (17% vs. 30%; p=0.47). The most common secondary alterations included *TERT* promoter mutations (33% PTC HGF vs. 30% PDTC; p=1.0) and *TP53* mutations (33% PTC HGF vs. 15% PDTC; p=0.22). Among segmental CNA, relative gain of 1q was a common event in both tumor types, occurring in 67% of PTC HGF and 15% of PDTC (p=0.0017).

Conclusions: Our results demonstrate that PTC HGF are important to recognize based on their aggressive behavior. The molecular differences between PTC HGF and PDTC suggest that PTC HGF should potentially be considered as a distinct group.

608 Defining Crucial Pathologic Parameters in Thyroid Neoplasm Using 3D Whole Block Imaging (WBI) with Micro resolution CT scanner (MicroCT): A Proof of Concept

Bin Xu[1], Alexei Teplov[1], Kareem Ibrahim[1], Takashi Inoue[2], Benjamin Stueben[1], Nora Katabi[1], Meera Hameed[1], Ronald Ghossein[1], Yukako Yagi[1]

[1]Memorial Sloan Kettering Cancer Center, New York, NY, [2]Memorial Sloan Kettering Cancer Center, Shunan, Yamaguchi, Japan

Disclosures: Bin Xu: None; Alexei Teplov: None; Kareem Ibrahim: None; Takashi Inoue: None; Benjamin Stueben: None; Nora Katabi: None; Meera Hameed: None; Ronald Ghossein: None; Yukako Yagi: None

Background: In the modern era, detailed pathologic characteristics of a thyroid tumor are crucial to achieve accurate diagnosis and guide treatment. The presence of capsular invasion (CI) distinguishes malignant tumors from their benign counterparts, whereas the presence and extent of vascular invasion (VI) and the size of nodal metastasis (NM) are included in risk stratification to assess the need for radioactive iodine therapy. However, the very definition of CI and VI is surrounded by controversies and an accurate assessment of NM is lacking. Whole Block Imaging (WBI) by microCT is a new imaging modality to create 3D reconstruction of whole tissue block with microscopic level resolution potentially up to 10x without the need for tissue sectioning. In this study, we aimed to define CI, VI, and NM volume using WBI. by microCT of paraffin blocks (PB).

Design: Twenty-seven PBs from 26 thyroid tumors (including 11 papillary carcinomas, 7 Hurthle cell carcinomas, 7 noninvasive follicular thyroid neoplasms with papillary-like nuclear features, and 2 PBs from 1 follicular carcinoma) were scanned using a custom-build Nikon Metrology microCT scanner. Ten PBs contained CI, whereas 7 PBs had VI. The data were reconstructed into 3D volumetric images. Images were compared with whole slide images (WSI) of corresponding H&E slides. In 2 cases with VI and/or CI, WSI of serial H&E slides were obtained and underwent 3D-reconstruction to be compared with the WBI.

Results: 1) Satellite tumor nodules beyond tumor capsule were shown to be CI by demonstrating the point of penetration using microCT and 3D reconstruction (Figure 1). 2) Additional foci of CI were detected in WBI using microCT. 3) VI was best defined as endothelialized tumor embolus within a vascular space. Associated fibrin thrombus was not always present on serially sectioned H&E slides. 4) WBI by microCT scanner was able to assess the volume of NM.

Figure 1 - 608

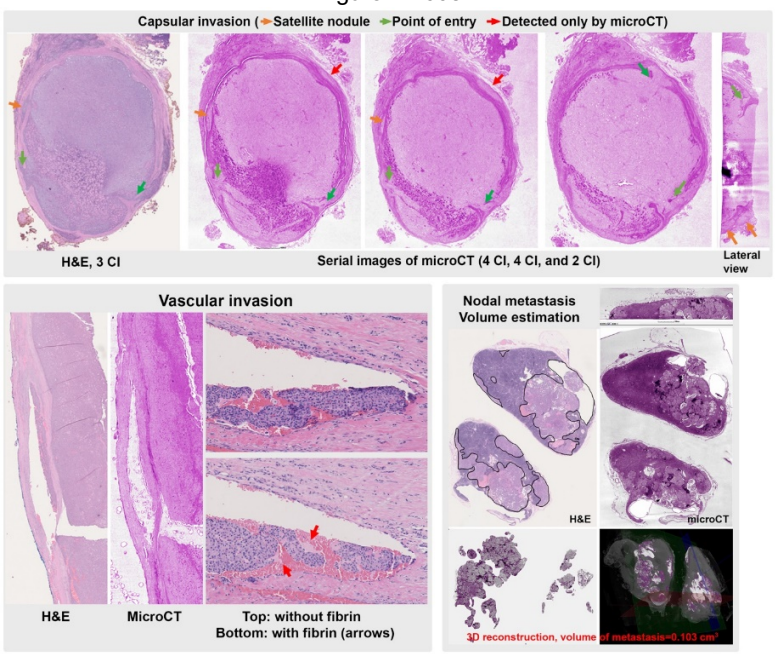

Conclusions: WBI by microCT scanner is able to detect CI, VI, and volume of NM in thyroid carcinoma. It has the potential to increase the detection rate of invasion, better define criteria for CI and VI and provide an accurate assessment of the volume of nodal disease.

609 Dissecting Anaplastic Thyroid Carcinoma (ATC): A Comprehensive Clinicohistologic, Immunophenotypic, and Molecular Studies of 357 Cases

Bin Xu[1], Talia Fuchs[2], Snjezana Dogan[1], Iñigo Landa[1], Nora Katabi[1], James Fagin[1], Eric Sherman[1], Anthony Gill[3], Ronald Ghossein[1]
[1]Memorial Sloan Kettering Cancer Center, New York, NY, [2]Royal North Shore Hospital, Sydney, NSW, Australia, [3]University of Sydney, Greenwich, NSW, Australia

Disclosures: Bin Xu: None; Talia Fuchs: None; Snjezana Dogan: None; Iñigo Landa: None; Nora Katabi: None; James Fagin: None; Eric Sherman: *Advisory Board Member*, Loxo; *Advisory Board Member*, Regeneron; Anthony Gill: None; Ronald Ghossein: None

Background: ATC is a devastating thyroid cancer that is nearly always fatal. However, large studies on ATC are exceedingly rare. We aimed to study the clinical, genotypic and phenotypic characteristics of ATC in the largest retrospective cohort of ATC to date.

Design: Three hundred and fifty-seven patients with ATC were gathered from 2 tertiary centers (MSKCC n=286, RNSH n=71). The slides were reviewed by 3 endocrine pathologists. Molecular testing was performed in 127 cases including 108 using next generation sequencing.

Results: The median patients' age was 68 (range: 29-99). The predominant morphology of ATC was spindle cell (26%), pleomorphic (23%), squamous cell carcinoma (21%), epithelioid (19%), rhabdoid (8%), and osteoclast giant cell-rich (3%). Differentiated thyroid carcinoma (DTC) was present in 205 cases (57%), the most common being papillary carcinoma (n=147). In primary resection of ATC, tumor infiltration, microscopic extrathyroidal extension (ETE), gross ETE, positive margin, gross residual disease and nodal metastasis were noted in 93%, 86%, 92%, 79%, 35% and 56% of cases. ATCs were frequently positive for PAX8 (67%), occasionally positive for TTF-1 (27%), whereas nearly always negative for thyroglobulin (98%).

The 1-year, 2-year, 3-year, and 5-year overall survival (OS) was 39%, 21%, 16%, and 14% respectively. On univariate analysis, patient's age at ATC diagnosis, the presence of DTC, resectability, margin status, nodal metastasis, encapsulation, gross residual disease, gross ETE, Percentage and size of ATC in the primary tumor, chemotherapy, and radiation therapy predicted OS ($p<0.05$). Age and gross residual disease were the only independent prognostic factors on multivariate analysis (Cox proportion model, $p<0.05$).

BRAF^{V600E} and *RAS* mutations were detected in 54 and 33 patients and did not correlate with outcome. *TERT* promoter, *TP53, PIK3CA, E1F1AX, PTEN, NF2, NF1, and KMT2D* mutations were detected in 79%, 63%, 17%, 15%, 13%, 12%, 10%, and 10% of ATC respectively, none of which impacted OS. 12 cases had pure squamous cell carcinoma without pre/co-existing DTC, all of which carried *BRAF*^{V600E} mutation and showed a similar OS compared with other ATCs ($p=0.781$).

Conclusions: It is crucial for pathologists to report encapsulation, margin, percentage and size of ATC in the primary tumor as they seem to be prognostically relevant. Pure squamous cell carcinoma of thyroid may be considered as ATC given its association with *BRAF*^{V600E} mutation and similar outcome.

610 Parasitic Thyroid Nodules or Metastatic Thyroid Carcinoma? Lessons Learned from Immunohistochemistry

Evgeny Yakirevich[1], Mikhail Gorbounov[2], Veronica Ulici[2], Sonja Chen[1], Li Juan Wang[3], Ronald Delellis[1], Diana Treaba[4]
[1]Rhode Island Hospital, Providence, RI, [2]Rhode Island Hospital/Brown University, Providence, RI, [3]Alpert Medical School of Brown University, Providence, RI, [4]Brown University Lifespan Academic Medical Center, Providence, RI

Disclosures: Evgeny Yakirevich: None; Mikhail Gorbounov: None; Veronica Ulici: None; Sonja Chen: None; Li Juan Wang: None; Ronald Delellis: None; Diana Treaba: None

Background: Parasitic nodules (PN) are defined as nodules of non-neoplastic thyroid tissue separate from the main thyroid gland. PN have been described in nodular or diffuse hyperplasia and lymphocytic thyroiditis. Distinguishing PN with lymphocytic thyroiditis from neck lymph nodes (LN) involved by metastatic papillary thyroid carcinoma (PTC) may be challenging. We aimed to evaluate the utility of IHC for endothelial markers in order to distinguish PN from LN.

Design: We searched our institutional archives between 2000-2019 to identify 11 cases diagnosed as PN. Corresponding orthotopic thyroid specimens were also retrieved. Paraffin-embedded whole tissue sections were analyzed for IHC expression of CD31, CD34, ERG, D2-40, and Factor VIII. For comparison, 10 non-neoplastic neck LN, and 10 neck LN involved by metastatic PTC were stained.

Results: Among 11 cases with PN, there were 8 females and 3 males, with a median age of 49 years. FNA was performed in 6 cases, with suspicion for PTC in 2 cases, and oncocytic neoplasm in one. In 10 cases the nodules were referred to pathology as level 6 LN, and in one as a level 3 LN. Frozen sections from neck nodules were performed in 6 cases: 3 were interpreted as benign; the 3 other were deferred. The size of the PN varied from 0.3 cm to 2.0 cm. Microscopically, 8 PN showed lymphocytic thyroiditis, and 3 nodular hyperplasia. Seven cases of lymphocytic thyroiditis were preceded by total thyroidectomy, revealing PTC in 2 cases, micro PTC in a background of lymphocytic thyroiditis in 3 cases, and sclerosing variant of lymphocytic thyroiditis in 2 cases in the orthotopic thyroid. All

endothelial markers highlighted vascular endothelium in PN and all markers except D2-40 stained high endothelial venules in LN. In addition, in non-neoplastic LN and in LN involved by metastatic PTC, CD31 IHC highlighted subcapsular and corticomedullary sinuses in a continuous linear pattern with positively stained histiocytes in cases of sinus histiocytosis. ERG showed nuclear immunoreactivity highlighting sinuses, while patchy staining was observed with D2-40 and sinuses were not stained with CD34 or Factor VIII.

Figure 1 - 610

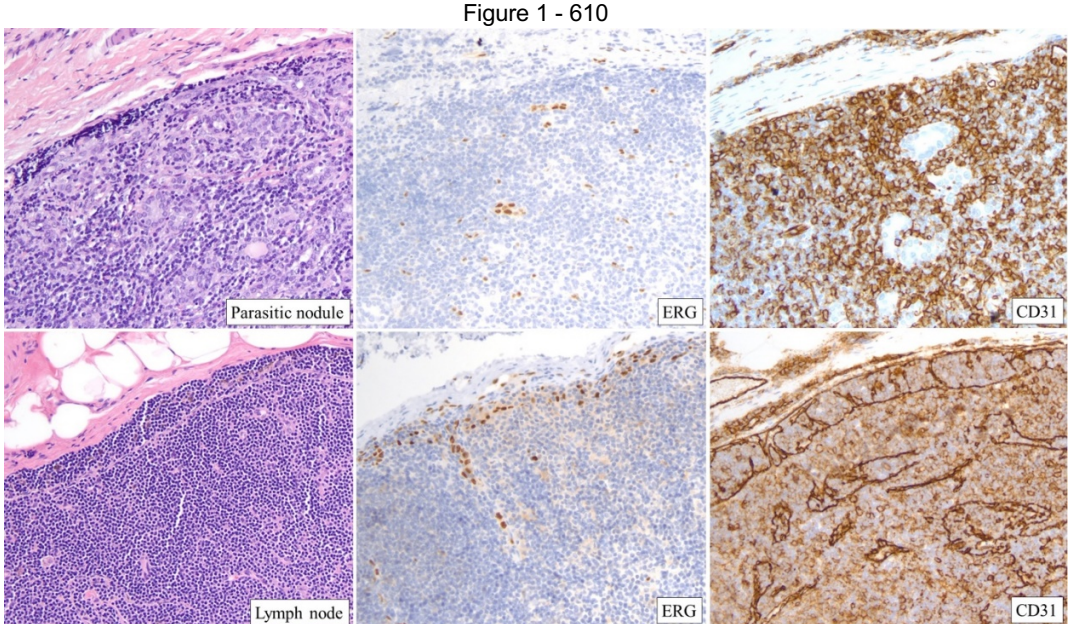

Conclusions: In this series, PN were seen predominantly in mid-age females most commonly in the setting of lymphocytic thyroiditis. PN can mimic LN metastases from PTC clinically, can raise suspicion for PTC or oncocytic neoplasm on FNA, and may be challenging on frozen and permanent sections. IHC for CD31 and ERG may be helpful in distinguishing PN from their mimics.

611 Diagnostic Value of the Cell Block Technique in the Diagnosis of Thyroid Nodules by Fine Needle Aspiration

Pablo Zoroquiain[1], Carlos Misad[1], Freddy Caques[1], Antonieta Alejandra Solar González[2]
[1]Pontificia Universidad Catolica de Chile, Santiago, RM, Chile, [2]Pontificia Universidad Catolica de Chile, Santiago, Región Metropolitana, Chile

Disclosures: Pablo Zoroquiain: None; Carlos Misad: None; Freddy Caques: None; Antonieta Alejandra Solar González: None

Background: Cytologic evaluation of fine needle aspiration (FNA) biopsy is the most accurate test to evaluate thyroid nodules (TN). Since 2007, the Bethesda System (BS), developed for cytologic smears evaluation, has been used to homogenize nomenclature and predict the risk of malignancy (RoM) of TN. Moreover, in several centers FNA material has been evaluated using only the cell block (CB) technique, but its diagnostic value has not been assessed in larger series. The aim of this study is to analyze the diagnostic value of the CB to evaluate TN by FNA without smears.

Design: All FNA samples from 2011 to 2018, evaluated by CB without smears, with an excisional biopsy available, were analyzed. A cyto-histologic correlation was determined using the histologic material as gold standard. Sensitivity (Se), Specificity (SP), Negative predictive Value (NPV) and positive predictive value (PPV) were calculated to evaluate the diagnostic value for neoplasia and malignancy as previously reported.

Results: A total of 1381 thyroid nodules from 1210 patients were found. Mean age was 44.2±14.4 years; 84.7% were women and 15.3% men. According to the BS: 37.2% were category VI; 19.4%, V; 19.3%, IV; 6.0%, III; 14.9%, II and 3.1%, I. Using only CB, the RoM was 99.0%, 95.5%, 25.1%, 30.1%, 3.8% and 16.2%, for VI, V, IV, III, II and I, respectively. Se, Sp, PPV and NPV of the CB for neoplasia diagnosis was 97.4%, 74%, 93.9% and 87.4%; and for malignancy 98.3%, 98.5%, 99.4% and 95.6%, respectively.

Conclusions: The CB has a good diagnostic value to evaluate neoplasia and malignancy in TN, and is similar to what has been reported previously using smears. Moreover, it has a good overall adequacy rate. These results, in addition to the capability to perform immunohistochemistry in the same sample make this technique a valuable and useful alternative to the conventional smear.